In this paper, we describe an algorithm for approximating functions of the form $f(x) = \int_a^b x^\mu \sigma(\mu)\, d\mu$ over $[0,1] \subset \mathbb{R}$, where $0 < a < b < \infty$ and $\sigma(\mu)$ is some signed Radon measure over $[a,b]$ or some distribution supported on $[a,b]$. Given the desired accuracy ϵ and the values of a and b, our method determines a priori a collection of non-integer powers $\{t_j\}_{j=1}^N$, so that the functions are approximated by series of the form $f(x) \approx \sum_{j=1}^N c_j x^{t_j}$, where the expansion coefficients can be found by solving a square, low-dimensional Vandermonde-like linear system using the collocation points $\{x_j\}_{j=1}^N$, also determined a priori by ϵ and the values of a and b. We prove that our method has a small uniform approximation error which is proportional to ϵ multiplied by some small constants. We demonstrate the performance of our algorithm with several numerical experiments, and show that the number of singular powers and collocation points grows as $N = O(\log \frac{1}{\epsilon})$.

On the Approximation of Singular Functions by Series of Non-integer Powers

Mohan Zhao[†◇] and Kirill Serkh[‡◇]
University of Toronto NA Technical Report
August 20, 2023

◇ This author's work was supported in part by the NSERC Discovery Grants RGPIN-2020-06022 and DGECR-2020-00356.

† Dept. of Computer Science, University of Toronto, Toronto, ON M5S 2E4
Corresponding author. Email: mohan.zhao@mail.utoronto.ca

‡ Dept. of Math. and Computer Science, University of Toronto, Toronto, ON M5S 2E4
Email: kserkh@math.toronto.edu

Keywords: *approximation theory, singular functions, singular value decompositions, corners, endpoint singularities, Laplace transforms, partial differential equations*

1 Introduction

The approximation of functions with singularities is a central topic in approximation theory. One motivating application is the representation of solutions to partial differential equations (PDEs) on nonsmooth geometries or with discontinuous data, which are known to be characterized by power-type singularities. Substantial progress has been made in this area, and existing methods can be classified into several categories, the primary ones being rational approximation, Sinc approximation combined with single- or double-exponential transformations, methods incorporating a priori knowledge of singularity types, and function approximation using combinations of complex exponentials obtained from the c-eigenpairs of certain Hankel matrices.

Rational approximation is a classical and well-established method for approximating functions with singularities, using rational basis functions determined by their poles and residues or by their weights in barycentric representations. In 1964, Newman discovered that there exists a rational approximation to the function $f(x) = |x|$ on $[-1, 1]$, converging at a rate of $O(\exp(-C\sqrt{n}))$ [21] (the polynomial approximation to $|x|$ on $[-1, 1]$ can only achieve a convergence rate no better than $O(n^{-1})$). Furthermore, he observed that the same approximation also applies to the functions $f(x) = \sqrt{x}$ and $f(x) = x^{\alpha}$ on $[0, 1]$. It is noteworthy that Newman's approximation utilizes poles that are clustered exponentially and symmetrically around zero along the imaginary axis.

Numerous papers have been published on rational approximation methods for functions with singularities since Newman's discovery (see, for example, [8], [26], [18], [6]). The best possible rational approximation is the so-called minimax approximation, which minimizes the maximum uniform approximation error between the function and its rational approximation. However, this minimax approximation is not easily to find and is not necessarily unique in the complex plane [11]. In practice, it turns out that the poles of the rational approximation can often be determined a priori, similar to those employed in Newman's method, to achieve a root-exponential convergence rate. One such method is Stenger's approximation [28], which involves interpolating the functions at a set of preassigned points exponentially clustered near the endpoints of the interval, in a rational basis with poles that are exponentially clustered at the endpoints.

While Stenger's method uses explicit formulas for the rational approximations, the residues can also be found numerically. In fact, if the poles are determined a priori, one can oversample the function and use the least-squares method to determine the residues which minimize the maximum approximation error. A class of methods utilizing this technique is known as lightning methods, which have been designed to approximate solutions of Laplace ([10], [9]) and Helmholtz ([9]) equations on two-dimensional domains with corners. Lightning methods employ rational functions with preassigned poles that cluster exponentially around the corner singularities along rays. It was proved in [10] that any complex poles exhibiting exponential clustering, with spacing scaling as $O(n^{-1/2})$, can achieve root-exponential rates of convergence. On more general geometries, the adaptive Antoulas-Anderson (AAA) algorithm [20] is an efficient and flexible nonlinear method that was developed to be domain-independent. The AAA method employs rational barycentric representations in the real or complex plane, incrementally increases the approximation order during iterations, and dynamically selects poles using a greedy algorithm. To determine the weights in the rational barycentric representations, the algorithm likewise solves a least-squares problem at each iteration.

While all the aforementioned methods can achieve root-exponential rates of convergence, it was discovered in [30] that further improvements in convergence rates can be obtained for most methods with preassigned poles by employing poles with tapered exponential clustering around singularities, such that the clustering density on a logarithmic scale tapers off linearly to zero near the singularities.

Rational approximation can also be applied after a change of variables. An approach referred to as reciprocal-log approximation [19] uses approximations of the form $r(\log z)$, where $r(s)$ is a rational function with poles determined a priori, either on a parabolic contour or confluent at the same point. Similarly to lightning methods, the coefficients are determined through a linear least-squares problem using collocation points that cluster exponentially around $z = 0$. This method converges at a rate of $O(\exp(-Cn))$ or $O(\exp(-Cn/\log n))$, depending on the form of the approximation and the function's behaviour in the complex plane.

An alternative approach is to use a combination of a change of variables and an approximation scheme that converges rapidly for smooth functions on the real line. By applying smooth transformations to functions with singularities at the endpoints of some finite intervals on the real line, these functions can be transformed into rapidly decaying functions, with the singularities mapped to the point at infinity. After this transformation, such functions can be approximated accurately using the Sinc approximation, by a truncated Sinc expansion. Two primary approaches of this type have been developed: the SE-Sinc and DE-Sinc approximations (see, for example, [27], [22] and [17]). The SE-Sinc approximation combines the single-exponential transformation with the Sinc approximation, resulting in a convergence rate of $O(\exp(-C\sqrt{n}))$, while the DE-Sinc approximation combines the double-exponential transformation with the Sinc approximation, to further improve the convergence rate to $O(\exp(-Cn/\log n))$.

While the previously mentioned methods can approximate functions with unknown singularity types, an alternative approach is possible when the leading terms of the singular functions are known in advance. In such cases, the singularities can be included directly in the approximation scheme. This often occurs in the solutions of boundary value problems for PDEs on domain with corners, when asymptotic expansions of the singularities around corners are available. It was revealed in [15] that the solutions of the Dirichlet problem for linear second order elliptic PDEs have singular expansions in terms of the form $r^\alpha(r^q \log r)^m$, where r is the radial distance from the singularity, $\alpha \in \mathbb{R}$, $q, m \in \mathbb{N}$ and $q \geq 1$. It was shown in [29] that, when singularities are of the type r^α, the rates of convergence of ordinary finite element methods are limited by the order α, even when the order of the polynomial basis is high. As pointed out in [29], a common method to reduce the error of approximation is by including the leading terms of the singularities into the interpolation basis of finite element methods, over sufficiently large regions around the singular points. One example of a method of this kind is the Blended Singular Basis Function Method (BSBFM) [23], in which the basis functions of elements in regions near the singular points are augmented with singular basis functions, constructed from leading-order singular powers multiplied by one-zone or two-zone blending functions. An alternative approach which also uses the leading terms of singularities is known as the method of auxiliary mapping (MAM) (see, for example, [16], [1]). MAM addresses the corner singularities by employing conformal mappings on neighborhoods of corners, so that the solutions on the transformed neighborhoods become more regular. When

PDEs are reformulated as integral equations for boundary charge or dipole densities used to represent the solutions, leading terms of the asymptotic expansions of the singular densities can likewise be used in the approximation scheme. Such approximations were taken in [24] and [25] to solve the Laplace and Helmholtz equations.

Following a different approach, Beylkin and Monzón [4] proposed a method that involves representing a function by a linear combination of exponential terms with complex-valued exponents and coefficients. This method is motivated by the observation that many functions admit representations by exponential integrals over contours in the complex plane, which can then be discretized by quadrature. Instead of starting with a contour integral however, the existence of such representations is only assumed implicitly, and the exponents (which they also call nodes) are obtained by finding the roots of a c-eigenpolynomial corresponding to a Hankel matrix, constructed from uniform samples of the function over the interval, while the coefficients (or weights) are determined via a Vandermonde system. We note that their primary focus is on minimizing the error at the sample points, and for singular functions, they only emphasize the error on a subinterval which excludes the singularities.

In this paper, we present a method for approximating functions with an endpoint singularity over $[0,1] \subset \mathbb{R}$, or more generally, a curve $\Gamma \subset \mathbb{C}$, where the functions have the form $f(x) = \int_a^b x^\mu \sigma(\mu)\, d\mu$, where $0 < a < b < \infty$, $x \in [0,1]$, and $\sigma(\mu)$ is some signed Radon measure over $[a,b]$ or some distribution supported on $[a,b]$. Our method represents these functions as expansions of the form $\widehat{f}_N(x) = \sum_{j=1}^N \widehat{c}_j x^{t_j}$, so that $\|f - \widehat{f}_N\|_{L^\infty[0,1]} \approx \epsilon$, where the singular powers $\{t_j\}_{j=1}^N$ are determined a priori based on the desired approximation accuracy ϵ and the values of a and b. The coefficients of the expansion are determined by solving a Vandermonde-like collocation problem

$$\begin{pmatrix} x_1^{t_1} & x_1^{t_2} & \dots & x_1^{t_N} \\ x_2^{t_1} & x_2^{t_2} & \dots & x_2^{t_N} \\ \vdots & \vdots & \ddots & \vdots \\ x_N^{t_1} & x_N^{t_2} & \dots & x_N^{t_N} \end{pmatrix} \begin{pmatrix} c_1 \\ c_2 \\ \vdots \\ c_N \end{pmatrix} = \begin{pmatrix} f(x_1) \\ f(x_2) \\ \vdots \\ f(x_N) \end{pmatrix} \tag{1}$$

for $f(x)$ at the points $\{x_j\}_{j=1}^N$, which are likewise determined a priori by ϵ, a and b. We show that these collocation points cluster tapered-exponentially near the singularities at $x = 0$. We also show numerically that, in order to obtain a uniform approximation error of ϵ, the number of basis functions and collocation points grows as $N = O(\log \frac{1}{\epsilon})$. Our method does not require any prior knowledge of the singularity types, besides the values of a and b, and the resulting basis functions depend only on these values, together with the precision ϵ. In contrast to rational approximation which converges only at a root-exponential rate, our method converges exponentially. When compared to the DE-Sinc approximation method which requires a large number of collocation points placed at the both endpoints after applying the smooth transformation (even when singularities only happen at only one endpoint), and reciprocal-log approximation which uses many collocation points together with least squares, our method has a small number both of basis functions and collocation points, such that the coefficients can be determined via a square, low-dimensional Vandermonde-like system.

Among all the methods discussed, the methodology of Beylkin and Monzón [4] bears the closest similarity with our method. However, unlike their method, our method emphasizes achieving a small uniform error over the entire interval.

The structure of this paper is as follows. Section 2 reviews the truncated Laplace transform and the truncated singular value decomposition. Section 3 demonstrates some numerical findings about the singular value decomposition of the truncated Laplace transform. Section 4 develops the main analytical tools of this paper. Section 5 describes some numerical experiments which provide conditions for the practical use of the theorems in section 4. Section 6 shows that functions of the form $f(x) = \int_a^b x^\mu \sigma(\mu)\, d\mu$ can be approximated uniformly by expansions in singular powers. Section 7 shows that the coefficients of such expansions can be obtained numerically by solving a Vandermonde-like system, and provides a bound for the uniform approximation error. Section 8 illustrates that the previous results can be extended to the case where the measure is replaced by a distribution. Section 9 shows that, in practice, the algorithm can be applied using a smaller number of basis functions and collocation points than stated in section 7. Finally, section 10 presents several numerical experiments to demonstrate the performance of our algorithm.

2 Mathematical Preliminaries

In this section, we provide some mathematical preliminaries.

2.1 The Truncated Laplace Transform

Throughout this paper, we utilize the analytical and numerical properties of the truncated Laplace transform, which have been previously presented in [13]. Here, we briefly review the key properties.

For a function $f(x) \in L^2[a,b]$, where $0 < a < b < \infty$, the truncated Laplace transform $\mathcal{L}_{a,b}$ is a linear mapping $L^2[a,b] \to L^2[0,\infty)$, defined by the formula

$$(\mathcal{L}_{a,b}(f))(x) = \int_a^b e^{-xt} f(t)\, dt. \tag{2}$$

We introduce the operator $T_\gamma \colon L^2[0,1] \to L^2[0,\infty)$, defined by the formula

$$(T_\gamma(f))(x) = \int_0^1 e^{-x(t+\frac{1}{\gamma-1})} f(t)\, dt, \tag{3}$$

so that T_γ is the truncated Laplace transform of $f(x)$ shifted from $[a,b]$ to $[0,1]$, where $\gamma = \frac{b}{a}$. It is clear that $\mathcal{L}_{a,b}$ and T_γ are compact operators (see, for example [3]).

As pointed out in [13], the singular value decomposition of the operator T_γ consists of an orthonormal sequence of right singular functions $\{u_i\}_{i=0,1,\ldots,\infty} \in L^2[0,1]$, an orthonormal sequence of left singular functions $\{v_i\}_{i=0,1,\ldots,\infty} \in L^2[0,\infty)$, and a discrete sequence of singular values $\{\alpha_i\}_{i=0,1,\ldots,\infty} \in \mathbb{R}$. The operator T_γ can be rewritten as

$$(T_\gamma(f))(x) = \sum_{i=0}^{\infty} \alpha_i \Big(\int_0^1 u_i(t) f(t)\, dt \Big) v_i(x), \tag{4}$$

for any function $f(x) \in L^2[0,1]$. Note that

$$T_\gamma(u_i) = \alpha_i v_i, \tag{5}$$

and

$$T_\gamma^*(v_i) = \alpha_i u_i, \tag{6}$$

for all $i = 0, 1, \ldots,$ where T_γ^* is the adjoint of T_γ, defined by

$$(T_\gamma^*(g))(t) = \int_0^\infty e^{-x(t+\frac{1}{\gamma-1})} g(x)\,dx. \tag{7}$$

Furthermore, for all $i = 0, 1, \ldots,$

$$\alpha_i > \alpha_{i+1} \geq 0, \tag{8}$$

and $\{\alpha_i\}_{i=0,1,\ldots,\infty}$ decays exponentially fast in n.

Assume that the left singular functions of $\mathcal{L}_{a,b}$ are denoted by $\widetilde{v}_0, \widetilde{v}_1, \ldots,$ and that the right singular functions of $\mathcal{L}_{a,b}$ are denoted by $\widetilde{u}_0, \widetilde{u}_1, \ldots$. Then, the relations between the singular functions of $\mathcal{L}_{a,b}$ and those of T_γ are given by the formulas

$$u_i(t) = \sqrt{b-a}\; \widetilde{u}_i(a + (b-a)t), \tag{9}$$

and

$$v_i(x) = \frac{1}{\sqrt{b-a}}\; \widetilde{v}_i(\frac{x}{b-a}), \tag{10}$$

for all $i = 0, 1, \ldots$. It is observed in [13] that $\widetilde{v}_0, \widetilde{v}_1, \ldots$ are the eigenfunctions of the 4th order differential operator $\widehat{D}_\omega$, defined by

$$\Big(\widehat{D}_\omega(f)\Big)(\omega) = -\frac{\mathrm{d}^2}{\mathrm{d}\omega^2}\left(\omega^2 \frac{\mathrm{d}^2}{\mathrm{d}\omega^2} f(\omega)\right) + (a^2+b^2)\frac{\mathrm{d}}{\mathrm{d}\omega}\left(\omega^2 \frac{\mathrm{d}}{\mathrm{d}\omega} f(\omega)\right) + (-a^2b^2\omega^2 + 2a^2) f(\omega), \tag{11}$$

where $f \in C^4[0,\infty) \cap L^2[0,\infty)$, and that $u_0, u_1, \ldots$ are the eigenfunctions of the 2nd order differential operator $\widetilde{D}_t$, defined by

$$\Big(\widetilde{D}_t(f)\Big)(t) = \frac{\mathrm{d}}{\mathrm{d}t}\left((t^2-a^2)(b^2-t^2)\frac{\mathrm{d}}{\mathrm{d}t} f(t)\right) - 2(t^2-a^2) f(t), \tag{12}$$

where $f \in C^2[a,b]$. Thus, $\widetilde{v}_i$, for all $i = 0, 1, \ldots,$ can be evaluated by finding the solution to the differential equation

$$-\frac{\mathrm{d}^2}{\mathrm{d}\omega^2}\left(\omega^2 \frac{\mathrm{d}^2}{\mathrm{d}\omega^2} \widetilde{v}_i(\omega)\right) + (a^2+b^2)\frac{\mathrm{d}}{\mathrm{d}\omega}\left(\omega^2 \frac{\mathrm{d}}{\mathrm{d}\omega} \widetilde{v}_i(\omega)\right) + (-a^2b^2\omega^2 + 2a^2)\widetilde{v}_i(\omega) = \widehat{\chi}_i \widetilde{v}_i(\omega), \tag{13}$$

where $\widehat{\chi}_i$ is the ith eigenvalue of the differential operator $\widehat{D}_\omega$. Similarly, $\widetilde{u}_i$, for all $i = 0, 1, \ldots,$ can be evaluated by finding the solution to the differential equation

$$\frac{\mathrm{d}}{\mathrm{d}t}\left((t^2-a^2)(b^2-t^2)\frac{\mathrm{d}}{\mathrm{d}t} \widetilde{u}_i(t)\right) - 2(t^2-a^2)\widetilde{u}_i(t) = \widetilde{\chi}_i \widetilde{u}_i(t), \tag{14}$$

where $\widetilde{\chi}_i$ is the ith eigenvalue of the differential operator $\widetilde{D}_t$.

A procedure for the evaluation of the singular functions and singular values of the operator T_γ, as well as the roots of the singular functions, is described comprehensively in [13].

2.2 The Truncated Singular Decomposition (TSVD)

The singular value decomposition (SVD) of a matrix $A \in \mathbb{R}^{m \times n}$ is defined by

$$A = U\Sigma V^T, \tag{15}$$

where the left and right matrices $U \in \mathbb{R}^{m\times m}$ and $V \in \mathbb{R}^{n \times n}$ are orthogonal, and the matrix $\Sigma \in \mathbb{R}^{m\times n}$ is a diagonal matrix with the singular values of A on the diagonal, in descending order, so that

$$\Sigma = \mathrm{diag}(\sigma_1, \sigma_2, \ldots, \sigma_{\min\{m,n\}}). \tag{16}$$

Let $r \leq \min\{m, n\}$ denote the rank of A, which is equal to the number of nonzero entries on the diagonal, and suppose that $k \leq r$. The k-truncated singular value decomposition (k-TSVD) of A is defined as

$$A_k = U\Sigma_k V^T, \tag{17}$$

where

$$\Sigma_k = \mathrm{diag}(\sigma_1, \ldots, \sigma_k, 0, \ldots, 0) \in \mathbb{R}^{m\times n}. \tag{18}$$

The pseudo-inverse of A_k is defined by

$$A_k^\dagger = V\Sigma_k^\dagger U^T \in \mathbb{R}^{n\times m}, \tag{19}$$

where

$$\Sigma_k^\dagger = \mathrm{diag}({\sigma_1}^{-1}, \ldots, {\sigma_k}^{-1}, 0, \ldots, 0) \in \mathbb{R}^{n\times m}. \tag{20}$$

The following theorem bounds the sizes of the solution and residual, when a perturbed linear system is solved using the TSVD. It follows the same reasoning as the proof of Theorem 3.4 in [12].

Theorem 2.1. *Suppose that $A \in \mathbb{R}^{m\times n}$, where $m \geq n$, and let $\sigma_1 \geq \sigma_2 \geq \cdots \geq \sigma_n$ be the singular values of A. Suppose that $x \in \mathbb{R}^n$ satisfies*

$$Ax = b. \tag{21}$$

Let $\epsilon > 0$, and suppose that

$$\widehat{x}_k = (A + E)_k^\dagger (b + e), \tag{22}$$

where $(A + E)_k^\dagger$ is the pseudo-inverse of the k-TSVD of $A + E$, so that

$$\widehat{\sigma}_k \geq \epsilon \geq \widehat{\sigma}_{k+1}, \tag{23}$$

where $\widehat{\sigma}_k$ and $\widehat{\sigma}_{k+1}$ are the kth and $(k + 1)$th largest singular values of $A + E$, and where $E \in \mathbb{R}^{m\times n}$ and $e \in \mathbb{R}^m$, with $\|E\|_2 < \epsilon/2$. Then

$$\|\widehat{x}_k\|_2 \leq \frac{1}{\widehat{\sigma}_k}(2\epsilon\|x\|_2 + \|e\|_2) + \|x\|_2. \tag{24}$$

and

$$\|A\widehat{x}_k - b\|_2 \leq 5\epsilon\|x\|_2 + \frac{3}{2}\|e\|_2. \tag{25}$$

Proof. Let $\sigma_1 \geq \sigma_2 \geq \cdots \geq \sigma_n$ denote the singular values of A, and let A_k be the k-TSVD of A. We observe that $A_k x = b - (A - A_k)x$. Letting $r_k = (A - A_k)x$ denote the residual, we see that $\|r_k\|_2 \leq \sigma_{k+1}\|x\|_2$ and that $b - A_k x = r_k$. Let $x_k = A_k^{\dagger} b$. Clearly, $b - Ax_k = r_k$ and $\|x_k\|_2 \leq \|x\|_2$.

Let $\widehat{A} := A + E$. We see that

$$
\begin{aligned}
\widehat{x}_k &= \widehat{A}_k^{\dagger}(b+e) \\
&= \widehat{A}_k^{\dagger}(Ax_k + r_k + e) \\
&= \widehat{A}_k^{\dagger}(\widehat{A}x_k - Ex_k + r_k + e) \\
&= \widehat{A}_k^{\dagger}(-Ex_k + r_k + e) + \widehat{A}_k^{\dagger}\widehat{A}x_k \\
&= \widehat{A}_k^{\dagger}(-Ex_k + r_k + e) + \widehat{A}_k^{\dagger}\widehat{A}_k x_k.
\end{aligned} \tag{26}
$$

Taking norms on both sides and observing that $\widehat{A}_k^{\dagger}\widehat{A}_k$ is an orthogonal projection,

$$
\begin{aligned}
\|\widehat{x}_k\|_2 &\leq \|\widehat{A}_k^{\dagger}\|_2(\|E\|_2\|x_k\|_2 + \|e\|_2 + \|r_k\|_2) + \|x_k\|_2 \\
&\leq \|\widehat{A}_k^{\dagger}\|_2(\|E\|_2\|x_k\|_2 + \|e\|_2 + \sigma_{k+1}\|x\|_2) + \|x_k\|_2.
\end{aligned} \tag{27}
$$

Letting $\widehat{\sigma}_1 \geq \widehat{\sigma}_2 \geq \cdots \geq \widehat{\sigma}_n$ denote the singular values of $A+E$, we have by the Bauer-Fike Theorem (see [2]) that $|\widehat{\sigma}_j - \sigma_j| \leq \|E\|_2$ for $j = 1, 2, \ldots, n$. Since $\widehat{\sigma}_k \geq \epsilon \geq \widehat{\sigma}_{k+1}$ and $\|E\|_2 < \epsilon/2$, we see that $\sigma_{k+1} < 3\epsilon/2$. Therefore,

$$
\begin{aligned}
\|\widehat{x}_k\|_2 &\leq \frac{1}{\widehat{\sigma}_k}\left(\frac{\epsilon}{2}\|x\|_2 + \|e\|_2 + \frac{3\epsilon}{2}\|x\|_2\right) + \|x\|_2 \\
&= \frac{1}{\widehat{\sigma}_k}(2\epsilon\|x\|_2 + \|e\|_2) + \|x\|_2.
\end{aligned} \tag{28}
$$

To bound the residual, we observe that

$$
\begin{aligned}
A\widehat{x}_k - b &= A\widehat{x}_k - Ax_k - r_k \\
&= A(\widehat{x}_k - x_k) - r_k \\
&= \widehat{A}(\widehat{x}_k - x_k) - E(\widehat{x}_k - x_k) - r_k.
\end{aligned} \tag{29}
$$

From (26), we have that

$$
\widehat{x}_k - x_k = \widehat{A}_k^{\dagger}(-Ex_k + r_k + e) - (I - \widehat{A}_k^{\dagger}\widehat{A}_k)x_k. \tag{30}
$$

Combining these two formulas,

$$
\begin{aligned}
A\widehat{x}_k - b &= \widehat{A}\widehat{A}_k^{\dagger}(-Ex_k + r_k + e) - \widehat{A}(I - \widehat{A}_k^{\dagger}\widehat{A}_k)x_k - E(\widehat{x}_k - x_k) - r_k \\
&= \widehat{A}_k\widehat{A}_k^{\dagger}(-Ex_k + r_k + e) - \widehat{A}(I - \widehat{A}_k^{\dagger}\widehat{A}_k)x_k - E(\widehat{x}_k - x_k) - r_k \\
&= \widehat{A}_k\widehat{A}_k^{\dagger}(-Ex_k + e) - \widehat{A}(I - \widehat{A}_k^{\dagger}\widehat{A}_k)x_k - E(\widehat{x}_k - x_k) - (I - \widehat{A}_k\widehat{A}_k^{\dagger})r_k.
\end{aligned} \tag{31}
$$

Since $\widehat{A}(I - \widehat{A}_k^{\dagger}\widehat{A}_k) = (\widehat{A} - \widehat{A}_k)(I - \widehat{A}_k^{\dagger}\widehat{A}_k)$, we see that

$$
A\widehat{x}_k - b = \widehat{A}_k\widehat{A}_k^{\dagger}(-Ex_k + e) - (\widehat{A} - \widehat{A}_k)(I - \widehat{A}_k^{\dagger}\widehat{A}_k)x_k - E(\widehat{x}_k - x_k) - (I - \widehat{A}_k\widehat{A}_k^{\dagger})r_k. \tag{32}
$$

Taking norms on both sides and observing that $\widehat{A}_k \widehat{A}_k^\dagger$ and $(I - \widehat{A}_k^\dagger \widehat{A}_k)$ are orthogonal projections,

$$\begin{aligned}
\|A\widehat{x}_k - b\|_2 &\le 2\|E\|_2\|x_k\|_2 + \|e\|_2 + \widehat{\sigma}_{k+1}\|x_k\|_2 + \|E\|_2\|\widehat{x}_k\|_2 + \|r_k\|_2 \\
&\le \frac{7}{2}\epsilon\|x\|_2 + \|e\|_2 + \frac{1}{2}\epsilon\|\widehat{x}_k\|_2 \\
&\le 5\epsilon\|x\|_2 + \frac{3}{2}\|e\|_2. \qquad (33)
\end{aligned}$$

■

3 Numerical Apparatus

In this section, we present several numerical experiments to examine some numerical properties of the singular value decomposition of the shifted truncated Laplace transform, T_γ. These findings are critical in the later proofs. We make the following observations:

1. The straight lines displayed in fig. 1 indicate that the singular values of T_γ decay exponentially.
2. Figure 2a and fig. 3a show that the L^∞ norm of both the left and right singular functions remains small, even for large values of γ.
3. Suppose that $x_1, x_2, \ldots, x_n$ are the roots of $v_n(x)$, and that $t_1, t_2, \ldots, t_n$ are the roots of $u_n(t)$. Let the weights $w_1, w_2, \ldots, w_n$ and $\widetilde{w}_1, \widetilde{w}_2, \ldots, \widetilde{w}_n$ satisfy

$$\int_0^\infty v_i(x)\,dx = \sum_{k=1}^n w_k v_i(x_k), \qquad (34)$$

   and

$$\int_0^1 u_i(t)\,dt = \sum_{k=1}^n \widetilde{w}_k u_i(t_k), \qquad (35)$$

   for all $i = 0, 1, \ldots, n-1$. Then the weights are all positive.
4. Figure 2b and fig. 3b show that the sizes of weights defined in eq. (34) and eq. (35) are small.

4 Analytical Apparatus

In this section, we present the principal analytical tools of this paper.

The following theorem states that the products of any two functions in the range of the operator T_γ, introduced in section 2.1, can be expressed as a function in the range of T_γ, after a change of variable.

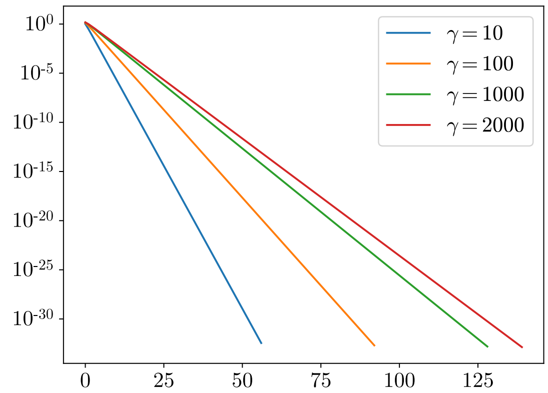

Figure 1: The singular values α_i of T_γ

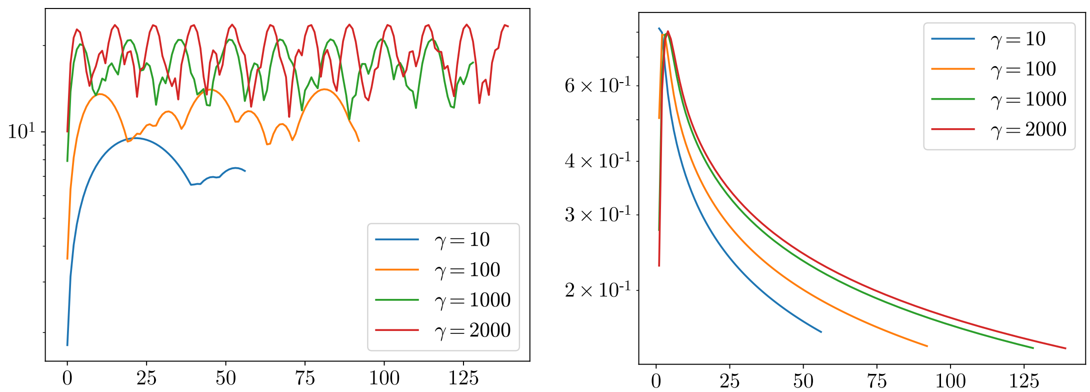

(a) $\|u_i\|_{L^\infty[a,b]}$ (b) $\|\widetilde{w}\|_2$

Figure 2

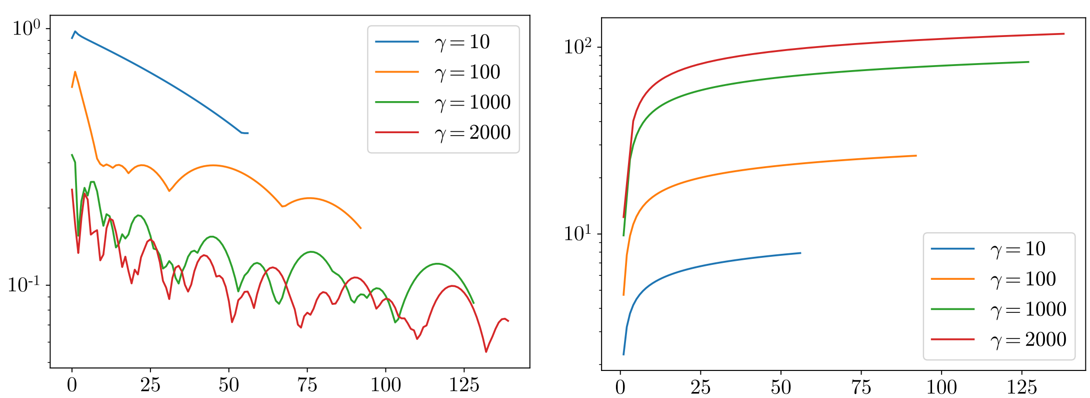

(a) $\|v_i\|_{L^\infty[0,\infty)}$ (b) $\max_j \sqrt{w_j}$

Figure 3

Theorem 4.1. *Suppose that the functions p, $q \in L^2[0,\infty)$ are defined by*

$$p(x) = \int_0^1 e^{-x(t+\frac{1}{\gamma-1})}\eta(t)\,dt, \tag{36}$$

and

$$q(x) = \int_0^1 e^{-x(t+\frac{1}{\gamma-1})}\varphi(t)\,dt, \tag{37}$$

respectively, for some η*,* $\varphi \in L^2[0,1]$*, and some* $\gamma > 1$*. Then, there exists some* $\sigma \in L^2[0,1]$*, such that*

$$p(x)\cdot q(x) = \int_0^1 e^{-x(2t+\frac{2}{\gamma-1})}\sigma(t)\,dt. \tag{38}$$

Proof. For any p and q defined by eq. (36) and eq. (37), we have

$$\begin{aligned} p(x)\cdot q(x) &= \int_0^1 e^{-x(t+\frac{1}{\gamma-1})}\eta(t)\,dt \int_0^1 e^{-x(s+\frac{1}{\gamma-1})}\varphi(s)\,ds \\ &= \int_0^1\int_0^1 e^{-x(t+s+\frac{2}{\gamma-1})}\eta(t)\varphi(s)\,ds\,dt. \end{aligned} \tag{39}$$

Defining a new variable $u = t+s$ and changing the range of integration, eq. (39) becomes

$$\begin{aligned} p(x)\cdot q(x) = \int_0^1 & e^{-x(u+\frac{2}{\gamma-1})}\int_0^u \eta(u-s)\varphi(s)\,ds\,du \\ &+ \int_1^2 e^{-x(u+\frac{2}{\gamma-1})}\int_{u-1}^1 \eta(u-s)\varphi(s)\,ds\,du. \end{aligned} \tag{40}$$

Letting $v = \frac{u}{2}$, we have

$$\begin{aligned} p(x)\cdot q(x) &= \int_0^{\frac{1}{2}} e^{-x(2v+\frac{2}{\gamma-1})}\int_0^{2v}\eta(2v-s)\varphi(s)\,ds\,2dv \\ &\qquad + \int_{\frac{1}{2}}^1 e^{-x(2v+\frac{2}{\gamma-1})}\int_{2v-1}^1 \eta(2v-s)\varphi(s)\,ds\,2dv \\ &= \int_0^1 e^{-x(2v+\frac{2}{\gamma-1})}\sigma(v)\,dv, \end{aligned} \tag{41}$$

where

$$\sigma(v) = 2\int_0^{2v}\eta(2v-s)\varphi(s)\,ds, \tag{42}$$

for $v \in [0,\frac{1}{2}]$, and

$$\sigma(v) = 2\int_{2v-1}^1 \eta(2v-s)\varphi(s)\,ds, \tag{43}$$

for $v \in [\frac{1}{2},1]$. ■

Observation 4.1. Suppose we have nodes x_1, x_2, …, x_n and weights w_1, w_2, …, w_n, such that

$$\Big|\int_0^\infty \int_0^1 e^{-x(t+\frac{1}{\gamma-1})}\eta(t)\,dt\,dx - \sum_{j=1}^n w_j \int_0^1 e^{-x_j(t+\frac{1}{\gamma-1})}\eta(t)\,dt\Big| < \epsilon\|\eta\|_{L^2[0,1]}, \tag{44}$$

for any $\eta \in L^2[0,1]$. Notice that

$$\begin{aligned}&\int_0^\infty p(x)\cdot q(x)\,dx\\ =&\int_0^\infty p(\frac{u}{2})\cdot q(\frac{u}{2})\cdot\frac{1}{2}\,du\\ =&\int_0^\infty \frac{1}{2}\int_0^1 e^{-u(t+\frac{1}{\gamma-1})}\sigma(t)\,dt\,du.\end{aligned} \tag{45}$$

Thus,

$$\Big|\int_0^\infty p(x)\cdot q(x)\,dx - \sum_{j=1}^n \frac{w_j}{2}\cdot p(\frac{x_j}{2})\cdot q(\frac{x_j}{2})\Big| < \frac{1}{2}\epsilon\|\sigma\|_{L^2[0,1]} \le \epsilon\|\eta\|_{L^2[0,1]}\|\varphi\|_{L^2[0,1]}. \tag{46}$$

This theorem shows that the products of any two functions in the range of T_γ^*, can be expressed as a function in the range of T_γ^*.

Theorem 4.2. *Suppose that the functions $p, q \in L^2[0,1]$ are defined by*

$$p(t) = \int_0^\infty e^{-x(t+\frac{1}{\gamma-1})}\eta(x)\,dx, \tag{47}$$

and

$$q(t) = \int_0^\infty e^{-x(t+\frac{1}{\gamma-1})}\varphi(x)\,dx, \tag{48}$$

respectively, for some η, $\varphi \in L^2[0,\infty)$, and some $\gamma > 1$. Then, there exists some $\sigma \in L^2[0,\infty)$, such that

$$p(t)\cdot q(t) = \int_0^\infty e^{-x(t+\frac{1}{\gamma-1})}\sigma(x)\,dx. \tag{49}$$

Proof. For any p and q defined by eq. (47) and eq. (48), we have

$$\begin{aligned}p(t)\cdot q(t) &= \int_0^\infty e^{-\omega(t+\frac{1}{\gamma-1})}\eta(\omega)\,d\omega \int_0^\infty e^{-x(t+\frac{1}{\gamma-1})}\varphi(x)\,dx\\ &= \int_0^\infty\int_0^\infty e^{-(\omega+x)(t+\frac{1}{\gamma-1})}\eta(\omega)\varphi(x)\,dx\,d\omega.\end{aligned} \tag{50}$$

Defining $u = \omega + x$ and changing the range of integration, eq. (50) becomes

$$\begin{aligned}p(t)\cdot q(t) &= \int_0^\infty e^{-u(t+\frac{1}{\gamma-1})}\int_0^u \eta(\omega)\varphi(u-\omega)\,d\omega\,du\\ &= \int_0^\infty e^{-u(t+\frac{1}{\gamma-1})}\sigma(u)\,du,\end{aligned} \tag{51}$$

where

$$\sigma(u) = \int_0^u \eta(\omega)\varphi(u-\omega)\,d\omega, \tag{52}$$

for $u \in [0,\infty)$. ■

Observation 4.2. Suppose we have nodes $t_1, t_2, \ldots, t_n$ and weights $w_1, w_2, \ldots, w_n$, such that

$$\Big|\int_0^1 \int_0^\infty e^{-x(t+\frac{1}{\gamma-1})}\eta(x)\,dx\,dt - \sum_{j=1}^n w_j \int_0^\infty e^{-x(t_j+\frac{1}{\gamma-1})}\eta(x)\,dx\Big| < \epsilon\|\eta\|_{L^2[0,\infty)}, \tag{53}$$

for any $\eta \in L^2[0,\infty)$. Since $p(t)\cdot q(t)$ is in the range of T_γ^*, we have

$$\Big|\int_0^1 p(t)\cdot q(t)\,dt - \sum_{j=1}^n w_j \cdot p(t_j)\cdot q(t_j)\Big| < \epsilon\|\sigma\|_{L^2[0,\infty)} \leq \epsilon\|\eta\|_{L^2[0,\infty)}\|\varphi\|_{L^2[0,\infty)}. \tag{54}$$

Leveraging the multiplication rule established earlier, we demonstrate that the following quadrature rule accurately integrates the products of the kernel of T_γ and the right singular functions of T_γ.

Corollary 4.3. *Suppose that we have a quadrature rule to integrate $\alpha_i u_i \cdot \alpha_j u_j$ to within an error of ϵ, for all i and j such that $i, j = 0, 1, \ldots, n-1$. Suppose further that $t_1, t_2, \ldots, t_m$ are the quadrature nodes, and $w_1, w_2, \ldots, w_m$ are the quadrature weights. Then, the error of the quadrature rule applied to functions of the form $f(t) = e^{-x(t+\frac{1}{\gamma-1})}u_i(t)$, with $x \in [0,\infty)$, is roughly equal to*

$$\frac{\epsilon}{\alpha_i}\sum_{j=0}^{n-1}\|v_j\|_{L^\infty[0,\infty)} + \alpha_n \cdot \|v_n\|_{L^\infty[0,\infty)} \cdot \|u_n\|_{L^\infty[0,1]} \cdot \|u_i\|_{L^\infty[0,1]} \cdot \sum_{k=1}^m |w_k|. \tag{55}$$

Proof. Since $e^{-x(t+\frac{1}{\gamma-1})}$ can be written as

$$e^{-x(t+\frac{1}{\gamma-1})} = \sum_{i=0}^\infty v_i(x)\alpha_i u_i(t), \tag{56}$$

we have

$$
\begin{aligned}
&\int_0^1 e^{-x(t+\frac{1}{\gamma-1})}u_i(t)\,dt - \sum_{k=1}^m w_k e^{-x(t_k+\frac{1}{\gamma-1})}u_i(t_k)\\
&= \int_0^1 \Big(\sum_{j=0}^\infty v_j(x)\alpha_j u_j(t)\Big)u_i(t)\,dt - \sum_{k=1}^m w_k\Big(\sum_{j=0}^\infty v_j(x)\alpha_j u_j(t_k)\Big)u_i(t_k)\\
&= \int_0^1 v_i(x)\alpha_i u_i^2(t)\,dt - \sum_{k=1}^m w_k\Big(\sum_{j=0}^\infty v_j(x)\alpha_j u_j(t_k)\Big)u_i(t_k)\\
&= \int_0^1 v_i(x)\alpha_i u_i^2(t)\,dt - \Big(\sum_{j=0}^{n-1}\int_0^1 v_j(x)\alpha_j u_j(t)u_i(t)\,dt + \sum_{j=0}^{n-1} v_j(x)\alpha_j\Big(\frac{\epsilon}{\alpha_i\alpha_j}\Big)\\
&\qquad\qquad + \sum_{j=n}^\infty\sum_{k=1}^m w_k v_j(x)\alpha_j u_j(t_k)u_i(t_k)\Big)\\
&= -\Big(\sum_{j=0}^{n-1} v_j(x)\alpha_j\Big(\frac{\epsilon}{\alpha_i\alpha_j}\Big) + \sum_{j=n}^\infty\sum_{k=1}^m w_k v_j(x)\alpha_j u_j(t_k)u_i(t_k)\Big)\\
&= -\Big(\sum_{j=0}^{n-1} v_j(x)\frac{\epsilon}{\alpha_i} + \sum_{j=n}^\infty\sum_{k=1}^m w_k v_j(x)\alpha_j u_j(t_k)u_i(t_k)\Big).
\end{aligned}
\tag{57}
$$

Since $\{\alpha_i\}_{i=0,1,\dots,\infty}$ decays exponentially, we have

$$
\begin{aligned}
&\Big|\int_0^1 e^{-x(t+\frac{1}{\gamma-1})}u_i(t)\,dt - \sum_{k=1}^m w_k e^{-x(t_k+\frac{1}{\gamma-1})}u_i(t_k)\Big|\\
&\approx \Big|\sum_{j=0}^{n-1} v_j(x)\frac{\epsilon}{\alpha_i} + \sum_{k=1}^m w_k v_n(x)\alpha_n u_n(t_k)u_i(t_k)\Big|\\
&\le \frac{\epsilon}{\alpha_i}\sum_{j=0}^{n-1}\|v_j\|_{L^\infty[0,\infty)} + \sum_{k=1}^m |w_k|\cdot\alpha_n\cdot\|v_n\|_{L^\infty[0,\infty)}\cdot|u_n(t_k)|\cdot|u_i(t_k)|\\
&\le \frac{\epsilon}{\alpha_i}\sum_{j=0}^{n-1}\|v_j\|_{L^\infty[0,\infty)} + \alpha_n\cdot\|v_n\|_{L^\infty[0,\infty)}\cdot\|u_n\|_{L^\infty[0,1]}\cdot\|u_i\|_{L^\infty[0,1]}\cdot\sum_{k=1}^m|w_k|.
\end{aligned}
\tag{58}
$$

■

Suppose that $x_1, x_2, \dots, x_m$ and $w_1, w_2, \dots, w_m$ are the nodes and weights of a quadrature rule which integrates $\alpha_i v_i \cdot \alpha_j v_j$, to within an error of ϵ, for $i, j = 0, 1, \dots, n-1$. The following theorem shows that, if the left singular functions $\{v_i\}_{i=0,1,\dots,n-1}$ of the operator T_γ, are used as interpolation basis, then, the interpolation matrix for the nodes $x_1, x_2, \dots, x_m$ is well conditioned, provided that the maximum error ϵ of integrating $\alpha_i v_i \cdot \alpha_j v_j$, for $i, j = 0, 1, \dots, n-1$, is sufficiently small.

Theorem 4.4. *Suppose that we have an m-point quadrature rule which integrates $\alpha_i v_i \cdot \alpha_j v_j$, to within an error of ϵ, for all $i, j = 0, 1, \dots, n-1$. Suppose further that $x_1, x_2,$*

$\ldots$, x_m are the quadrature nodes, and w_1, w_2, $\ldots$, w_m are the quadrature weights. Let the matrix $A \in \mathbb{R}^{m\times n}$ be given by the formula

$$A = \begin{pmatrix} v_0(x_1) & v_1(x_1) & \ldots & v_{n-1}(x_1) \\ v_0(x_2) & v_1(x_2) & \ldots & v_{n-1}(x_2) \\ \vdots & \vdots & \ddots & \vdots \\ v_0(x_m) & v_1(x_m) & \ldots & v_{n-1}(x_m) \end{pmatrix}, \tag{59}$$

and let the matrix W be the diagonal matrix with diagonal entries w_1, w_2, $\ldots$, w_m. We define the matrix $E = [e_{jk}]$ such that

$$E = I - A^T W A. \tag{60}$$

Then,

$$|e_{jk}| \leq \frac{\epsilon}{\alpha_{j-1}\alpha_{k-1}}. \tag{61}$$

Proof. From eq. (60), we have

$$e_{jk} = \delta_{jk} - \sum_{l=1}^{m} w_l v_{j-1}(x_l) v_{k-1}(x_l), \tag{62}$$

where $\delta_{jk} = 1$ if $j = k$, and $\delta_{jk} = 0$ otherwise. Then,

$$\begin{aligned} |e_{jk}| &= \Big|\delta_{jk} - \sum_{l=1}^{m} w_l \alpha_{j-1} v_{j-1}(x_l) \cdot \alpha_{k-1} v_{k-1}(x_l) \frac{1}{\alpha_{j-1}\alpha_{k-1}}\Big| \\ &\leq \Big|\delta_{jk} - \Big(\frac{1}{\alpha_{j-1}\alpha_{k-1}} \int_0^\infty \alpha_{j-1} v_{j-1}(x) \cdot \alpha_{k-1} v_{k-1}(x)\, dx - \frac{\epsilon}{\alpha_{j-1}\alpha_{k-1}}\Big)\Big| \\ &= \frac{\epsilon}{\alpha_{j-1}\alpha_{k-1}}. \end{aligned} \tag{63}$$

■

The following corollary establishes an upper bound on the norm of the pseudo-inverse $A^\dagger$ of the matrix A defined in eq. (59).

Corollary 4.5. *Suppose that we have a collection of quadrature nodes x_1, x_2, $\ldots$, x_m and quadrature weights w_1, w_2, $\ldots$, w_m, which integrate $\alpha_i v_i \cdot \alpha_j v_j$ to within an error of $\epsilon \leq \frac{\alpha_n^2}{2\sqrt{n}}$, for all $i, j = 0, 1, \ldots, n-1$. Let $A \in \mathbb{R}^{m\times n}$ be the matrix defined in eq. (59). Then,*

$$\|A^\dagger\|_2 < \sqrt{2} \max_{1\leq i\leq m} \sqrt{w_i}, \tag{64}$$

where $A^\dagger \in \mathbb{R}^{n\times m}$ is the pseudo-inverse of A.

Proof. Since w_1, w_2, $\ldots$, w_m are positive, it is reasonable to let $W^{\frac{1}{2}}$ denote a diagonal matrix with entries $\sqrt{w_1}$, $\sqrt{w_2}$, $\ldots$, $\sqrt{w_m}$. We define B such that $B = W^{\frac{1}{2}} A$. It follows by eq. (60) that $B^T B = I - E$. Since $e_{jk} < \frac{\epsilon}{\alpha_n^2}$, for all $j, k = 1, 2, \ldots, n$, we have

$\|E\|_2 < \frac{\epsilon}{\alpha_n^2}\sqrt{n}$. Let $\widetilde{\sigma}_1, \widetilde{\sigma}_2, \ldots, \widetilde{\sigma}_n$ denote the singular values of $B^T B$. Then, it can be shown that (see Theorem IIIa in [2])

$$|\widetilde{\sigma}_j - 1| \leq \|E\|_2 < \frac{\epsilon}{\alpha_n^2}\sqrt{n}, \tag{65}$$

for all $j = 1, 2, \ldots, n$. This means that

$$1 - \frac{\epsilon}{\alpha_n^2}\sqrt{n} < \widetilde{\sigma}_j < 1 + \frac{\epsilon}{\alpha_n^2}\sqrt{n}. \tag{66}$$

Letting $k = \min\{n, m\}$ and $\sigma_1, \sigma_2, \ldots, \sigma_k$ be the singular values of B, we have

$$\sqrt{1 - \frac{\epsilon}{\alpha_n^2}\sqrt{n}} < \sigma_j < \sqrt{1 + \frac{\epsilon}{\alpha_n^2}\sqrt{n}}. \tag{67}$$

Letting $B^\dagger$ be the pseudo-inverse of B, such that $B^\dagger B = I$, since $B = W^{\frac{1}{2}} A$, we have that $A^\dagger = B^\dagger W^{\frac{1}{2}}$. Thus,

$$\begin{aligned} \|A^\dagger\|_2 &\leq \|B^\dagger\|_2 \|W^{\frac{1}{2}}\|_2 \\ &< \frac{1}{\sqrt{1 - \frac{\epsilon}{\alpha_n^2}\sqrt{n}}} \cdot \max_{1 \leq i \leq m} \sqrt{w_i}. \end{aligned} \tag{68}$$

If we have $\epsilon \leq \frac{\alpha_n^2}{2\sqrt{n}}$, then eq. (68) implies that

$$\|A^\dagger\|_2 < \sqrt{2} \max_{1 \leq i \leq m} \sqrt{w_i}. \tag{69}$$

■

5 Empirical Bounds

In this section, we present several numerical experiments to demonstrate that the error of the quadrature rule described in corollary 4.3, applied to the function $f(t) = e^{-x(t + \frac{1}{\gamma - 1})} u_i(t)$, for $i = 0, 1, \ldots, n-1$, turns out to be smaller than the bound described in corollary 4.3. We also show that the norm of $A^\dagger \in \mathbb{R}^{n \times m}$ achieves the bound specified in corollary 4.5, for a quadrature rule which integrates $\alpha_i v_i \cdot \alpha_j v_j$, for $i, j = 0, 1, \ldots, n-1$, to an error that exceeds $\frac{\alpha_n^2}{2\sqrt{n}}$.

Suppose that the nodes $t_1, t_2, \ldots, t_n$ are the roots of $u_n(t)$, and that the weights $\widetilde{w}_1, \widetilde{w}_2, \ldots, \widetilde{w}_n$ satisfy

$$\int_0^1 u_i(t)\, dt = \sum_{k=1}^{n} \widetilde{w}_k u_i(t_k), \tag{70}$$

for $i = 0, 1, \ldots, n-1$. Applying observation 4.2, we have

$$\begin{aligned} E_1 := \max_{i,j} \Big| \int_0^1 \alpha_i u_i(t) \cdot \alpha_j u_j(t)\, dt - \sum_{k=1}^{n} \widetilde{w}_k \alpha_i u_i(t_k) \cdot \alpha_j u_j(t_k) \Big| \\ < \alpha_n \|v_j\|_{L^2[0,\infty)} \|v_i\|_{L^2[0,\infty)} = \alpha_n. \end{aligned} \tag{71}$$

However, numerical experiments for $\gamma = 10$, 100 and 200 demonstrate that the error of the quadrature rule in eq. (70), applied to $\alpha_i u_i \cdot \alpha_j u_j$, for $i, j = 0, 1, \ldots, n-1$, is smaller than α_n^2 in practice, as shown in figs. 4a, 5a and 6a. Thus, it can be inferred from corollary 4.3 that the error of such quadrature rule applied to the function $f(t) = e^{-x(t+\frac{1}{\gamma-1})} u_i(t)$, is approximately of the same size as α_n.

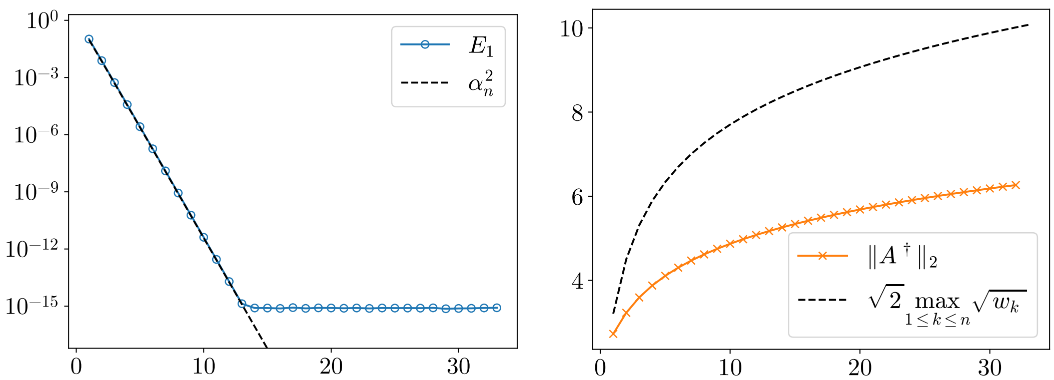

(a) (b)

Figure 4: $\gamma = 10$

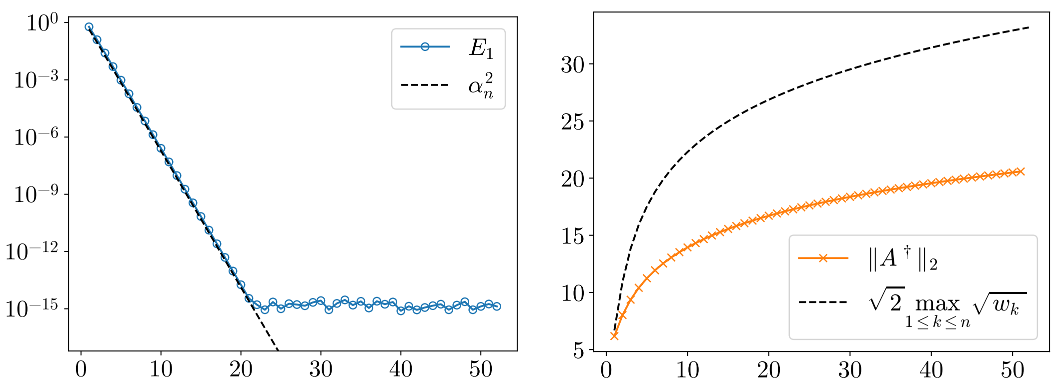

(a) (b)

Figure 5: $\gamma = 100$

Suppose that the nodes $x_1, x_2, \ldots, x_n$ are the roots of v_n, and the weights $w_1, w_2, \ldots, w_n$ satisfy

$$\int_0^\infty v_i(x)\, dx = \sum_{k=1}^n w_k v_i(x_k), \tag{72}$$

for $i = 0, 1, \ldots, n-1$. Observation 4.1 implies that

$$\begin{aligned} E_2 := \max_{i,j} \Big| \int_0^\infty \alpha_i v_i(x) \cdot \alpha_j v_j(x)\, dx - \sum_{k=1}^n \frac{w_k}{2} \alpha_i v_i(\frac{x_k}{2}) \cdot \alpha_j v_j(\frac{x_k}{2}) \Big| \\ < \alpha_n \|u_i\|_{L^2[0,1]} \|u_j\|_{L^2[0,1]} = \alpha_n \end{aligned} \tag{73}$$

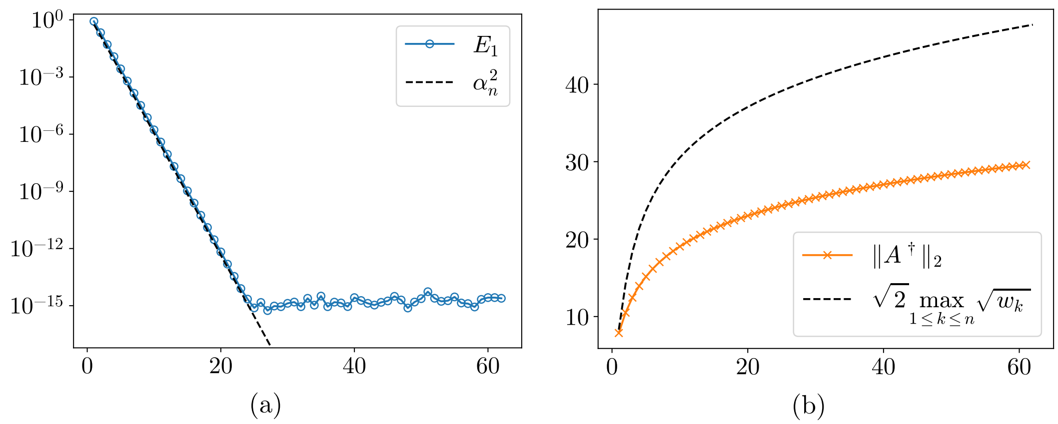

Figure 6: $\gamma = 200$

In contrast to the error of the quadrature rule in eq. (70) applied to $\alpha_i u_i \cdot \alpha_j u_j$, for $i, j = 0,\ 1,\ \ldots,\ n-1$, which is in practice less than α_n^2, the error of the quadrature rule in eq. (72) applied to $\alpha_i v_i \cdot \alpha_j v_j$, lies between α_n^2 and α_n. However, we observe that the special structure of $A \in \mathbb{R}^{n\times n}$ enables the norm of $A^\dagger$ to still attain the bound specified in eq. (64). The results for $\gamma = 10$, 100 and 200 are shown in figs. 4b, 5b and 6b, respectively.

Remark 5.1. It is worth emphasizing that the choice of quadrature nodes is not unique. Any set of quadrature nodes with corresponding weights that satisfy eq. (70) or eq. (72) can be employed for our purposes. In this paper, we choose the roots of u_n and v_n to be the quadrature nodes, since the associated weights are positive and reasonably small, which we have shown in section 3.

6 Approximation by Singular Powers

In this section, we present a method for approximating a function of the form

$$f(x) = \int_a^b x^\mu \sigma(\mu)\, d\mu, \qquad x \in [0,1], \tag{74}$$

for some signed Radon measure $\sigma(\mu)$, using a basis of $\{x^{t_j}\}_{j=1}^N$ for some specially chosen points $t_1,\ t_2,\ \ldots,\ t_N \in [a,b]$. Our approach involves an initial approximation using the left singular functions of T_γ, followed by a discretization of the left singular functions in terms of $\{x^{t_j}\}_{j=1}^N$.

In the following theorem, we establish the existence of such an approximation, and quantify its approximation error.

Theorem 6.1. *Let f be a function of the form eq. (74). Suppose that*

$$N \geq \min\{i : \alpha_i < {\alpha_n}^2\}. \tag{75}$$

Suppose further that $t_1,\ t_2,\ \ldots,\ t_N$ are the roots of u_N shifted to the interval $[a,b]$, and *that the weights $\widetilde{w}_1, \widetilde{w}_2, \ldots, \widetilde{w}_N$ satisfy*

$$\int_0^1 u_i(t)\,dt = \sum_{j=1}^{N} \widetilde{w}_j u_i\Big(\frac{t_j - a}{b-a}\Big), \tag{76}$$

for all $i = 0, 1, \ldots, N-1$. Then, there exists a vector $c \in \mathbb{R}^N$ such that the formula

$$f_N(x) = \sum_{j=1}^{N} c_j x^{t_j}, \tag{77}$$

satisfies

$$\begin{aligned}\|f - f_N\|_{L^\infty[0,1]} \le \alpha_n \cdot \|\sigma\|_{L^1[a,b]} \cdot \big(&\|u_n\|_{L^\infty[0,1]} \cdot \|v_n\|_{L^\infty[0,\infty)} \\ &+ n \max_{0\le i\le n-1} \|u_i\|_{L^\infty[0,1]} \cdot \frac{\max_{0\le i\le n-1} E_i}{\alpha_n}\big),\end{aligned} \tag{78}$$

where

$$E_i \le \alpha_n \sum_{j=0}^{n-1} \|v_j\|_{L^\infty[0,\infty)} + \alpha_n \cdot \|v_n\|_{L^\infty[0,\infty)} \cdot \|u_n\|_{L^\infty[0,1]} \cdot \|u_i\|_{L^\infty[0,1]} \cdot \sum_{l=1}^{N} |\widetilde{w}_l| \approx \alpha_n, \tag{79}$$

and the norm of the coefficient vector c is bounded by

$$\|c\|_2 \le \sqrt{\sum_{j=1}^{N} |\widetilde{w}_j|^2} \cdot \sqrt{N} n \cdot |\sigma| \cdot \big(\max_{0\le i\le n-1} \|u_i\|_{L^\infty[0,1]}\big)^2. \tag{80}$$

Proof. Substituting $\omega = -\log x$ into eq. (74), we have

$$\begin{aligned} f(e^{-\omega}) &= \int_a^b e^{-\omega\mu} \sigma(\mu)\,d\mu, \\ &= \int_0^1 e^{-\widetilde{\omega}(\bar{\mu} + \frac{1}{\gamma-1})} (b-a)\sigma((b-a)\bar{\mu} + a)\,d\bar{\mu}, \qquad \widetilde{\omega} \in [0,\infty), \end{aligned} \tag{81}$$

where $\bar{\mu} = \frac{\mu - a}{b-a}$, and $\widetilde{\omega} = (b-a)\omega$. Since $\{\alpha_i\}_{i=0,1,\ldots,\infty}$ decays exponentially, we truncate the SVD of the operator T_γ after n terms and obtain

$$e^{-\omega(t + \frac{1}{\gamma-1})} = \sum_{i=0}^{\infty} v_i(\omega)\alpha_i u_i(t) \approx \sum_{i=0}^{n-1} v_i(\omega)\alpha_i u_i(t). \tag{82}$$

Then, we construct the approximation $\widetilde{f}$ to f, defined by

$$\widetilde{f}(e^{-\widetilde{\omega}}) = \sum_{i=0}^{n-1} \alpha_i \bigg(\int_0^1 u_i(\bar{\mu})(b-a)\sigma((b-a)\bar{\mu} + a)\,d\bar{\mu}\bigg) v_i(\widetilde{\omega}). \tag{83}$$

Thus,

$$\begin{aligned}\widetilde{f}(x) &= \sum_{i=0}^{n-1} \alpha_i \bigg(\int_0^1 u_i(\bar{\mu})(b-a)\sigma((b-a)\bar{\mu}+a)\,d\bar{\mu} \bigg) v_i(-(b-a)\log x) \\ &= \sum_{i=0}^{n-1} \widetilde{c}_i \alpha_i v_i(-(b-a)\log x), \end{aligned} \tag{84}$$

for $x \in [0,1]$, where

$$\widetilde{c}_i = \int_0^1 u_i(\bar{\mu})(b-a)\sigma((b-a)\bar{\mu}+a)\,d\bar{\mu}, \tag{85}$$

for all $i = 0,\, 1,\, \ldots,\, n-1$. Due to Hölder's inequality, we observe that

$$|\widetilde{c}_i| \le |\sigma| \cdot \|u_i\|_{L^\infty[0,1]}, \tag{86}$$

and

$$\|\widetilde{c}\|_2 \le \sqrt{n}|\sigma| \cdot \max_{0\le i\le n-1} \|u_i\|_{L^\infty[0,1]}. \tag{87}$$

Thus,

$$\begin{aligned}\|f-\widetilde{f}\|_{L^\infty[0,1]} &= \Big\| \sum_{i=n}^{\infty} \widetilde{c}_i \alpha_i v_i(-(b-a)\log x) \Big\|_{L^\infty[0,1]} \\ &\approx \big\| \widetilde{c}_n \alpha_n v_n(-(b-a)\log x) \big\|_{L^\infty[0,1]} \\ &\le \alpha_n \cdot |\sigma| \cdot \|u_n\|_{L^\infty[0,1]} \cdot \|v_n\|_{L^\infty[0,\infty]}. \end{aligned} \tag{88}$$

According to eq. (5), we have

$$\alpha_i v_i(\omega) = \int_0^1 e^{-\omega(t+\frac{1}{\gamma-1})} u_i(t)\,dt. \tag{89}$$

Letting $t_1,\, t_2,\, \ldots,\, t_N$ be the roots of u_N, there exist some $\widetilde{w}_1,\, \widetilde{w}_2,\, \ldots,\, \widetilde{w}_N$, satisfying

$$\int_0^1 u_i(t)\,dt = \sum_{l=1}^{N} \widetilde{w}_l u_i(t_l), \tag{90}$$

for all $i = 0,\, 1,\, \ldots,\, N-1$. We apply observation 4.2 to obtain

$$\Big| \int_0^1 \alpha_i u_i(t) \alpha_j u_j(t)\,dt - \sum_{l=1}^{N} \widetilde{w}_l \alpha_i u_i(t_l) \alpha_j u_j(t_l) \Big| \le \alpha_N < {\alpha_n}^2, \tag{91}$$

for all $i, j = 0,\, 1,\, \ldots,\, n-1$. It follows from corollary 4.3 that

$$\begin{aligned} E_i &:= \Big| \int_0^1 e^{-\omega(t+\frac{1}{\gamma-1})} u_i(t)\,dt - \sum_{l=1}^{N} \widetilde{w}_l e^{-\omega(t_l+\frac{1}{\gamma-1})} u_i(t_l) \Big| \\ &< \alpha_n \sum_{j=0}^{n-1} \|v_j\|_{L^\infty[0,\infty)} + \alpha_n \cdot \|v_n\|_{L^\infty[0,\infty)} \cdot \|u_n\|_{L^\infty[0,1]} \cdot \|u_i\|_{L^\infty[0,1]} \cdot \sum_{l=1}^{N} |\widetilde{w}_l|. \end{aligned} \tag{92}$$

Since $\sum_{l=1}^{N} |\widetilde{w}_l|$, $\|v_j\|_{L^\infty[0,\infty)}$ and $\|u_j\|_{L^\infty[0,1]}$ are small, for all $j = 0, 1, \ldots, n-1$, as shown in section 3, the discretization error, E_i, is approximately of the size α_n.

Recalling from eq. (84), we have

$$\begin{aligned}
\widetilde{f}(x) &= \sum_{i=0}^{n-1} \widetilde{c}_i \alpha_i v_i(-(b-a)\log x), \\
&\leq \sum_{i=0}^{n-1} \widetilde{c}_i \sum_{j=1}^{N} \widetilde{w}_j e^{-\widetilde{\omega}(t_j + \frac{1}{\gamma-1})} u_i(t_j) + \sum_{i=0}^{n-1} \widetilde{c}_i E_i \\
&= \sum_{i=0}^{n-1} \widetilde{c}_i \sum_{j=1}^{N} \widetilde{w}_j e^{-\widetilde{\omega}\bar{t}_j} u_i(\bar{t}_j - \frac{1}{\gamma-1}) + \sum_{i=0}^{n-1} \widetilde{c}_i E_i, \qquad (93)
\end{aligned}$$

where $\widetilde{\omega} = -(b-a)\log x$, and $\bar{t}_j = t_j + \frac{1}{\gamma-1}$, for all $j = 1, 2, \ldots, N$. Substituting $e^{-\widetilde{\omega}} = x^{(b-a)}$ into eq. (93), we define the approximation f_N to $\widetilde{f}$,

$$\begin{aligned}
f_N(x) &= \sum_{i=0}^{n-1} \widetilde{c}_i \sum_{j=1}^{N} \widetilde{w}_j u_i(\bar{t}_j - \frac{1}{\gamma-1}) x^{(b-a)\bar{t}_j}, \\
&:= \sum_{j=1}^{N} c_j x^{(b-a)\bar{t}_j}, \qquad x \in [0,1], \qquad (94)
\end{aligned}$$

where $c_j = \widetilde{w}_j \sum_{i=0}^{n-1} \widetilde{c}_i u_i(\bar{t}_j - \frac{1}{\gamma-1})$, for $j = 1, 2, \ldots, N$. For the sake of simplicity, we rename the nodes $(b-a)\bar{t}_1, (b-a)\bar{t}_2, \ldots, (b-a)\bar{t}_N$ to $t_1, t_2, \ldots, t_N$, and observe that $t_1, t_2, \ldots, t_N \in [a,b]$. By eq. (94) and eq. (87), we have

$$\begin{aligned}
\|c\|_2 &\leq \sqrt{\sum_{j=1}^{N} |\widetilde{w}_j|^2} \cdot \sqrt{N}\sqrt{n} \cdot \|\widetilde{c}\|_2 \max_{0 \leq i \leq n-1} \|u_i\|_{L^\infty[0,1]} \\
&\leq \sqrt{\sum_{j=1}^{N} |\widetilde{w}_j|^2} \cdot \sqrt{N} n \cdot |\sigma| \cdot \big(\max_{0 \leq i \leq n-1} \|u_i\|_{L^\infty[0,1]}\big)^2. \qquad (95)
\end{aligned}$$

The approximation error of f_N to $\widetilde{f}$ can be bounded by

$$\begin{aligned}
\|\widetilde{f} - f_N\|_{L^\infty[0,1]} &\leq \Big\| \sum_{i=0}^{n-1} \widetilde{c}_i \max_{0 \leq i \leq n-1} E_i \Big\|_{L^\infty[0,1]} \\
&\leq \sqrt{n} \|\widetilde{c}\|_2 \max_{0 \leq i \leq n-1} E_i \\
&\leq n|\sigma| \cdot \max_{0 \leq i \leq n-1} \|u_i\|_{L^\infty[0,1]} \cdot \max_{0 \leq i \leq n-1} E_i. \qquad (96)
\end{aligned}$$

Thus, we obtain the bound on the approximation error of f_N to f as

$$\begin{aligned}
\|f - f_N\|_{L^\infty[0,1]} &\leq \|f - \widetilde{f}\|_{L^\infty[0,1]} + \|\widetilde{f} - f_N\|_{L^\infty[0,1]} \\
&\leq \alpha_n \cdot |\sigma| \cdot \big(\|u_n\|_{L^\infty[0,1]} \cdot \|v_n\|_{L^\infty[0,\infty)} \\
&\qquad + n \max_{0 \leq i \leq n-1} \|u_i\|_{L^\infty[0,1]} \cdot \frac{\max_{0 \leq i \leq n-1} E_i}{\alpha_n} \big). \qquad (97)
\end{aligned}$$

■

7 Numerical Algorithm and Error Analysis

In the previous section, we have showed that, given any function f of the form eq. (74), for each $N \geq \min\{i : \alpha_i < {\alpha_n}^2\}$, there exists a coefficient vector $c \in \mathbb{R}^N$ such that, when $t_1, t_2, \ldots, t_N$ are the roots of u_N shifted to the interval $[a, b]$,

$$f_N(x) = \sum_{j=1}^{N} c_j x^{t_j} \tag{98}$$

is uniformly close to f, to within an error given by eq. (78).

In this section, we show that, by letting $N = \min\{i : \alpha_i \leq \frac{{\alpha_n}^2}{2\sqrt{n}}\}$ and choosing the collocation points according to the formula

$$x_j = e^{-\frac{s_j}{b-a}}, \tag{99}$$

for $j = 1, 2, \ldots, N$, where $s_1, s_2, \ldots, s_N$ are the roots of v_N, we can construct an approximation

$$\widehat{f}_N(x) = \sum_{j=1}^{N} \widehat{c}_j x^{t_j} \tag{100}$$

which is also uniformly close to f, by solving a linear system

$$Vc = F, \tag{101}$$

for the coefficient vector $c \in \mathbb{R}^N$, where

$$V = \begin{pmatrix} x_1^{t_1} & x_1^{t_2} & \ldots & x_1^{t_N} \\ x_2^{t_1} & x_2^{t_2} & \ldots & x_2^{t_N} \\ \vdots & \vdots & \ddots & \vdots \\ x_N^{t_1} & x_N^{t_2} & \ldots & x_N^{t_N} \end{pmatrix} \in \mathbb{R}^{N \times N}, \tag{102}$$

and

$$F = (f(x_1), f(x_2), \ldots, f(x_N))^T \in \mathbb{R}^N. \tag{103}$$

The uniform approximation error of $\widehat{f}_N$ to f over $[0, 1]$ is bounded in theorem 7.3.

In the following lemma, we establish upper bounds on the norm and the residual of the perturbed TSVD solution $\widehat{c}$ to the linear system in eq. (101), in terms of the norm of the coefficient vector c in eq. (98).

Lemma 7.1. *Let $V \in \mathbb{R}^{N \times N}$, $F \in \mathbb{R}^N$, and $\epsilon > 0$. Suppose that*

$$\widehat{c}_k = (V + \delta V)_k^{\dagger}(F + \delta F), \tag{104}$$

where $(V + \delta V)_k^{\dagger}$ is the pseudo-inverse of the k-TSVD of $V + \delta V$, so that

$$\widehat{\alpha}_k \geq \epsilon \geq \widehat{\alpha}_{k+1}, \tag{105}$$

where $\widehat{\alpha}_k$ and $\widehat{\alpha}_{k+1}$ denote the kth and $(k+1)$th largest singular values of $V + \delta V$, where $\delta V \in \mathbb{R}^{N\times N}$ and $\delta F \in \mathbb{R}^N$, with

$$\|\delta V\|_2 \le \epsilon_0 \cdot \mu_1 < \frac{\epsilon}{2}, \tag{106}$$

and

$$\|\delta F\|_2 \le \epsilon_0 \cdot \mu_2. \tag{107}$$

Suppose further that

$$Vc = F + \Delta F, \tag{108}$$

for some $\Delta F \in \mathbb{R}^N$ and $c \in \mathbb{R}^N$. Then,

$$\|\widehat{c}_k\|_2 \le \frac{1}{\widehat{\alpha}_k}(2\epsilon + \widehat{\alpha}_k)\|c\|_2 + \frac{1}{\widehat{\alpha}_k}(\|\Delta F\|_2 + \epsilon_0 \cdot \mu_2), \tag{109}$$

and

$$\|V\widehat{c}_k - (F + \Delta F)\|_2 \le 5\epsilon\|c\|_2 + \frac{3}{2}\|\Delta F\|_2 + \frac{3}{2}\epsilon_0 \cdot \mu_2. \tag{110}$$

Proof. By eq. (104), we have

$$(V + \delta V)_k \widehat{c}_k = F + \delta F = F + \Delta F - \Delta F + \delta F = F + \Delta F + e, \tag{111}$$

where $e := -\Delta F + \delta F$. Thus, theorem 2.1 implies that

$$\begin{aligned}
\|\widehat{c}_k\|_2 &\le \frac{1}{\widehat{\alpha}_k}(2\epsilon + \widehat{\alpha}_k)\|c\|_2 + \frac{1}{\widehat{\alpha}_k}\|-\Delta F + \delta F\|_2 \\
&\le \frac{1}{\widehat{\alpha}_k}(2\epsilon + \widehat{\alpha}_k)\|c\|_2 + \frac{1}{\widehat{\alpha}_k}(\|\Delta F\|_2 + \epsilon_0 \cdot \mu_2),
\end{aligned} \tag{112}$$

and that

$$\|V\widehat{c}_k - (F + \Delta F)\|_2 \le 5\epsilon\|c\|_2 + \frac{3}{2}\|\Delta F\|_2 + \frac{3}{2}\epsilon_0 \cdot \mu_2. \tag{113}$$

■

The following observation bounds the backward error, $\|V\widehat{c}_k - F\|_2$, where $\widehat{c}_k$ is the TSVD solution to the perturbed linear system, defined in eq. (104).

Observation 7.1. According to lemma 7.1, the TSVD solution $\widehat{c}_k$ to the perturbed linear system is bounded by the norm of c, as described in eq. (109), where c is the exact solution to the linear system $Vc = F + \Delta F$, and satisfies eq. (80). Thus, the resulting backward error is bounded by

$$\begin{aligned}
\|V\widehat{c}_k - F\|_2 &= \big\|V\widehat{c}_k - \big(F + \Delta F\big) + \Delta F\big\|_2 \\
&\le \big\|V\widehat{c}_k - \big(F + \Delta F\big)\big\|_2 + \|\Delta F\|_2 \\
&\le 5\epsilon\|c\|_2 + \frac{5}{2}\|\Delta F\|_2 + \frac{3}{2}\epsilon_0 \cdot \mu_2.
\end{aligned} \tag{114}$$

Although the interpolation matrix V in the basis of $\{x^{t_j}\}_{j=1}^N$ tends to be ill-conditioned, resulting in a loss of stability in the solution to the linear system in eq. (101), we have shown in lemma 7.1 and observation 7.1 that, when the TSVD is used to solve the linear system in eq. (101), the backward error, $\|V\widehat{c}_k - F\|_2$, which measures the discrepancy between f and $\widehat{f}_N$ at the collocation points, is nonetheless small.

The following lemma bounds the L^∞-norm of a function of the form eq. (74), in terms of its values at the collocation points $\{x_j\}_{j=1}^N$. The constant appearing in this bound serves the same role as the Lebesgue constant for polynomial interpolation.

Lemma 7.2. *Let $N = \min\{i : \alpha_i \le \frac{\alpha_n{}^2}{2\sqrt{n}}\}$. Suppose that the collocation points $X := (x_j)_{j=1}^N$ are defined by the formula $x_j = e^{-\frac{s_j}{b-a}}$, where $s_1, s_2, \ldots, s_N$ are the roots of v_N, and that the weights $w_1, w_2, \ldots, w_N$ satisfy*

$$\int_0^\infty v_i(x)\,dx = \sum_{k=1}^N w_k v_i(x_k), \tag{115}$$

for $i = 0, 1, \ldots, N-1$. Let $f(x)$ be a function of the form eq. (74), for some signed Radon measure σ, and let $f(X) \in \mathbb{R}^N$ be the vector of values of $f(x)$ sampled at X. Then,

$$\begin{aligned}\|f\|_{L^\infty[0,1]} \le{}& \alpha_0\sqrt{2n}\cdot \max_{1\le j\le N}\sqrt{w_j}\cdot \max_{0\le i\le n-1}\|v_i\|_{L^\infty[0,\infty]}\cdot\|f(X)\|_2 \\ &+ \big(\alpha_n\cdot|\sigma|\cdot\|u_n\|_{L^\infty[0,1]}\cdot\|v_n\|_{L^\infty[0,\infty]}\big) \\ &\qquad\cdot\big(1+\alpha_0\sqrt{2n}\cdot\sqrt{N}\cdot\max_{1\le j\le N}\sqrt{w_j}\cdot\max_{0\le i\le n-1}\|v_i\|_{L^\infty[0,\infty]}\big).\end{aligned} \tag{116}$$

Proof. Recall from theorem 6.1 that $f(x)$ can be approximated by

$$\widetilde{f}(x) = \sum_{i=0}^{n-1}\widetilde{c}_i\alpha_i v_i(-(b-a)\log x), \tag{117}$$

such that

$$\|f-\widetilde{f}\|_{L^\infty[0,1]} \le \alpha_n\cdot|\sigma|\cdot\|u_n\|_{L^\infty[0,1]}\cdot\|v_n\|_{L^\infty[0,\infty]}. \tag{118}$$

Letting $\widetilde{f}(X) = \big(\widetilde{f}(x_1), \widetilde{f}(x_2), \ldots, \widetilde{f}(x_N)\big)^T$, since corollary 4.5 implies that $\|A^\dagger\|_2 < \sqrt{2}\max_{1\le j\le N}\sqrt{w_j}$, where the matrix $A^\dagger \in \mathbb{R}^{n\times N}$ is the pseudo-inverse of A, the coefficient vector $\widetilde{c}$ in eq. (117) can be found stably by the formula

$$\widetilde{c} = A^\dagger\widetilde{f}(X). \tag{119}$$

From eq. (117), we have

$$\begin{aligned}\|\widetilde{f}\|_{L^\infty[0,1]} &= \left\|\sum_{i=0}^{n-1}\widetilde{c}_i\alpha_i v_i(-(b-a)\log x)\right\|_{L^\infty[0,1]} \\ &\le \alpha_0\sqrt{n}\cdot\|\widetilde{c}\|_2\max_{0\le i\le n-1}\|v_i\|_{L^\infty[0,\infty]} \\ &\le \alpha_0\sqrt{n}\cdot\|A^\dagger\|_2\cdot\|\widetilde{f}(X)\|_2\max_{0\le i\le n-1}\|v_i\|_{L^\infty[0,\infty]} \\ &\le \alpha_0\sqrt{n}\cdot\sqrt{2}\cdot\max_{1\le j\le N}\sqrt{w_j}\cdot\|\widetilde{f}(X)\|_2\max_{0\le i\le n-1}\|v_i\|_{L^\infty[0,\infty]},\end{aligned} \tag{120}$$

where $w_1, w_2, \ldots, w_N$ are defined in eq. (115). Since

$$\left|f(x_j) - \widetilde{f}(x_j)\right| \le \|f - \widetilde{f}\|_{L^\infty[0,1]}, \tag{121}$$

for all $j = 1, 2, \ldots, N-1$, we have

$$\|\widetilde{f}(X)\|_2 \le \sqrt{N}\|f - \widetilde{f}\|_{L^\infty[0,1]} + \|f(X)\|_2. \tag{122}$$

It follows that

$$\begin{aligned}
\|f\|_{L^\infty[0,1]} &\le \|f - \widetilde{f}\|_{L^\infty[0,1]} + \|\widetilde{f}\|_{L^\infty[0,1]} \\
&\le \|f - \widetilde{f}\|_{L^\infty[0,1]} + \alpha_0\sqrt{n}\cdot\sqrt{2}\cdot \max_{1\le j\le N}\sqrt{w_j}\cdot\|\widetilde{f}(X)\|_2 \max_{0\le i\le n-1}\|v_i\|_{L^\infty[0,\infty]} \\
&\le \|f - \widetilde{f}\|_{L^\infty[0,1]} + \alpha_0\sqrt{n}\cdot\sqrt{2}\cdot \max_{1\le j\le N}\sqrt{w_j} \\
&\qquad\qquad \cdot\left(\sqrt{N}\|f - \widetilde{f}\|_{L^\infty[0,1]} + \|f(X)\|_2\right)\cdot \max_{0\le i\le n-1}\|v_i\|_{L^\infty[0,\infty]} \\
&\le \alpha_0\sqrt{2n}\cdot \max_{1\le j\le N}\sqrt{w_j}\cdot \max_{0\le i\le n-1}\|v_i\|_{L^\infty[0,\infty]}\cdot\|f(X)\|_2 \\
&\quad + \big(\alpha_n\cdot|\sigma|\cdot\|u_n\|_{L^\infty[0,1]}\cdot\|v_n\|_{L^\infty[0,\infty]}\big) \\
&\qquad\qquad \cdot\big(1 + \alpha_0\sqrt{2n}\cdot\sqrt{N}\cdot \max_{1\le j\le N}\sqrt{w_j}\cdot \max_{0\le i\le n-1}\|v_i\|_{L^\infty[0,\infty]}\big).
\end{aligned} \tag{123}$$

■

The following theorem provides an upper bound on the global approximation error of $\widehat{f}_N$ to f, when the coefficient vector in the approximation is computed by solving $Vc = F$ using the TSVD.

Theorem 7.3. *Let $f(x)$ be a function of the form eq. (74), for some signed Radon measure $\sigma(\mu)$. Suppose that $N = \min\{i : \alpha_i \le \frac{\alpha_n{}^2}{2\sqrt{n}}\}$. Let $t_1, t_2, \ldots, t_N$ be the roots of u_N shifted to the interval $[a,b]$, and let $x_1, x_2, \ldots, x_N$ be the collocation points defined by the formula $x_j = e^{-\frac{s_j}{b-a}}$, where $s_1, s_2, \ldots, s_N$ are the roots of v_N. Suppose $V \in \mathbb{R}^{N\times N}$ is defined in eq. (102) and $F \in \mathbb{R}^N$ is defined in eq. (103), and let $\epsilon > 0$. Suppose further that*

$$\widehat{c}_k = (V + \delta V)_k^\dagger (F + \delta F), \tag{124}$$

where $(V+\delta V)_k^\dagger$ is the pseudo-inverse of the k-TSVD of $V + \delta V$, so that

$$\widehat{\alpha}_k \ge \epsilon \ge \widehat{\alpha}_{k+1}, \tag{125}$$

where $\widehat{\alpha}_k$ and $\widehat{\alpha}_{k+1}$ denote the kth and $(k+1)$th largest singular values of $V + \delta V$, where $\delta V \in \mathbb{R}^{N\times N}$ and $\delta F \in \mathbb{R}^N$, with

$$\|\delta V\|_2 \le \epsilon_0\cdot\mu_1 < \frac{\epsilon}{2}, \tag{126}$$

and

$$\|\delta F\|_2 \le \epsilon_0\cdot\mu_2. \tag{127}$$

Let

$$\widehat{f}_N(x) = \sum_{j=1}^{N} \widehat{c}_{k,j} x^{t_j}, \tag{128}$$

with $\widehat{c}_k$ *defined in eq.* (124)*. Then,*

$$\|f - \widehat{f}_N\|_{L^\infty[0,1]} \lesssim \alpha_0 \cdot (\epsilon + \alpha_n + \frac{{\alpha_n}^2}{\widehat{\alpha}_k}) \cdot |\sigma| + \alpha_0 \epsilon_0 \mu_2 + \frac{\alpha_0 \alpha_n}{\widehat{\alpha}_k} \epsilon_0 \mu_2. \tag{129}$$

Proof. We observe that

$$\widehat{f}_N(x) = \int_a^b x^\mu \, \widehat{\sigma}_N(\mu) \, d\mu, \tag{130}$$

for the signed Radon measure,

$$\widehat{\sigma}_N(t) = \sum_{j=1}^{N} \widehat{c}_{k,j} \delta(t - t_j), \tag{131}$$

where $\delta(t)$ is the Dirac delta function. Then, $f(x) - \widehat{f}_N(x)$ can be rewritten as

$$f(x) - \widehat{f}_N(x) = \int_a^b x^\mu \big(\sigma(\mu) - \widehat{\sigma}_N(\mu)\big) \, d\mu, \tag{132}$$

where $\sigma(\mu)$ is defined in eq. (74). By theorem 6.1, there exists a vector $c \in \mathbb{R}^N$, such that

$$f_N(x) = \sum_{j=1}^{N} c_j x^{t_j} \tag{133}$$

is uniformly close to f, with an error bounded by eq. (78). Let $X := (x_j)_{j=1}^N$ and $\Delta F := f(X) - f_N(X)$. Notice that

$$\begin{aligned} \|\Delta F\|_2 &\le \sqrt{N} \cdot \|f - f_N\|_{L^\infty[0,1]} \\ &\le \alpha_n \cdot |\sigma| \cdot \sqrt{N} \Big(\|u_n\|_{L^\infty[0,1]} \cdot \|v_n\|_{L^\infty[0,\infty)} \\ &\qquad + n \cdot \max_{0 \le i \le n-1} \|u_i\|_{L^\infty[0,1]} \cdot \frac{\max_{0 \le i \le n-1} E_i}{\alpha_n} \Big). \end{aligned} \tag{134}$$

By eq. (114), we have

$$\begin{aligned} &\|f(X) - \widehat{f}_N(X)\|_2 \\ &= \|V \widehat{c}_k - F\|_2 \\ &\le 5\epsilon \|c\|_2 + \frac{5}{2} \|\Delta F\|_2 + \frac{3}{2} \epsilon_0 \cdot \mu_2 \\ &\le 5\epsilon \sqrt{\sum_{j=1}^{N} |\widetilde{w}_j|^2} \cdot \sqrt{N} n \cdot |\sigma| \cdot \big(\max_{0 \le i \le n-1} \|u_i\|_{L^\infty[0,1]} \big)^2 \\ &\qquad + \frac{5}{2} \alpha_n \cdot |\sigma| \cdot \sqrt{N} \, \Big(\|u_n\|_{L^\infty[0,1]} \cdot \|v_n\|_{L^\infty[0,\infty)} \\ &\qquad\qquad + n \cdot \max_{0 \le i \le n-1} \|u_i\|_{L^\infty[0,1]} \cdot \frac{\max_{0 \le i \le n-1} E_i}{\alpha_n} \Big) + \frac{3}{2} \epsilon_0 \cdot \mu_2, \end{aligned} \tag{135}$$

where $\widetilde{w}_1, \widetilde{w}_2, \ldots, \widetilde{w}_N$ are defined in eq. (76). Since, as shown in section 3, $\sqrt{\sum_{j=1}^{N} |\widetilde{w}_j|^2}$, $\|u_i\|_{L^\infty[0,1]}$ and $\|v_i\|_{L^\infty[0,\infty)}$ are all reasonably small, for $i = 0, 1, \ldots, n-1$, we have

$$\|f(X) - \widehat{f}_N(X)\|_2 \lesssim \epsilon|\sigma| + \alpha_n \cdot |\sigma| + \epsilon_0 \cdot \mu_2. \tag{136}$$

It follows from lemma 7.2 that the uniform error of the approximation of $\widehat{f}_N$ to f is roughly bounded as

$$\begin{aligned}
&\|f - \widehat{f}_N\|_{L^\infty[0,1]} \\
&\leq \alpha_0\sqrt{2n} \cdot \max_{1\leq j\leq N} \sqrt{w_j} \cdot \max_{0\leq i\leq n-1} \|v_i\|_{L^\infty[0,\infty]} \cdot \|f(X) - \widehat{f}_N(X)\|_2 \\
&\qquad + \big(\alpha_n \cdot |\sigma - \widehat{\sigma}_N| \cdot \|u_n\|_{L^\infty[0,1]} \cdot \|v_n\|_{L^\infty[0,\infty]}\big) \\
&\qquad\qquad \cdot \big(1 + \alpha_0\sqrt{2n} \cdot \sqrt{N} \cdot \max_{1\leq j\leq N} \sqrt{w_j} \cdot \max_{0\leq i\leq n-1} \|v_i\|_{L^\infty[0,\infty]}\big) \\
&\lesssim \alpha_0 \cdot \|f(X) - \widehat{f}_N(X)\|_2 + \alpha_n|\sigma - \widehat{\sigma}_N| \cdot \alpha_0 \\
&\lesssim \alpha_0 \cdot \big(\epsilon \cdot |\sigma| + \alpha_n \cdot |\sigma| + \epsilon_0 \cdot \mu_2 + \alpha_n|\sigma - \widehat{\sigma}_N|\big).
\end{aligned} \tag{137}$$

Since $|\sigma - \widehat{\sigma}_N| \leq |\sigma| + |\widehat{\sigma}_N|$ and $|\widehat{\sigma}_N| \leq \|\widehat{c}_k\|_1$, we have

$$\begin{aligned}
\|f - \widehat{f}_N\|_{L^\infty[0,1]} &\lesssim \alpha_0 \cdot (\epsilon + \alpha_n) \cdot |\sigma| + \alpha_0\epsilon_0\mu_2 + \alpha_0\alpha_n \cdot |\sigma| + \alpha_0\alpha_n \cdot \|\widehat{c}_k\|_1 \\
&\leq \alpha_0 \cdot (\epsilon + \alpha_n) \cdot |\sigma| + \alpha_0\epsilon_0\mu_2 + \alpha_0\alpha_n \cdot |\sigma| + \alpha_0\alpha_n \cdot \sqrt{N}\|\widehat{c}_k\|_2.
\end{aligned} \tag{138}$$

By ignoring the small terms in eq. (80) and eq. (134), eq. (112) becomes

$$\begin{aligned}
\|\widehat{c}_k\|_2 &\leq \frac{1}{\widehat{\alpha}_k}(2\epsilon + \widehat{\alpha}_k)\|c\|_2 + \frac{1}{\widehat{\alpha}_k}(\|\Delta F\|_2 + \epsilon_0 \cdot \mu_2) \\
&\approx \frac{1}{\widehat{\alpha}_k}(2\epsilon + \widehat{\alpha}_k)|\sigma| + \frac{1}{\widehat{\alpha}_k}(\alpha_n|\sigma| + \epsilon_0 \cdot \mu_2).
\end{aligned} \tag{139}$$

Thus, eq. (138) and eq. (139) imply that

$$\begin{aligned}
\|f - \widehat{f}_N\|_{L^\infty[0,1]} &\lesssim \alpha_0 \cdot (\epsilon + \alpha_n) \cdot |\sigma| + \alpha_0\epsilon_0\mu_2 + \alpha_0\alpha_n \cdot |\sigma| + \alpha_0\alpha_n \cdot \sqrt{N}\|\widehat{c}_k\|_2 \\
&\approx \alpha_0 \cdot (\epsilon + \alpha_n) \cdot |\sigma| + \alpha_0\epsilon_0\mu_2 + \alpha_0\alpha_n \cdot \|\widehat{c}_k\|_2 \\
&\approx \alpha_0 \cdot (\epsilon + \alpha_n + \frac{\alpha_n\epsilon}{\widehat{\alpha}_k} + \frac{\alpha_n^2}{\widehat{\alpha}_k}) \cdot |\sigma| + \alpha_0\epsilon_0\mu_2 + \frac{\alpha_0\alpha_n}{\widehat{\alpha}_k}\epsilon_0\mu_2.
\end{aligned} \tag{140}$$

Since $\widehat{\alpha}_k \geq \epsilon$, eq. (140) becomes

$$\|f - \widehat{f}_N\|_{L^\infty[0,1]} \lesssim \alpha_0 \cdot (\epsilon + \alpha_n + \frac{{\alpha_n}^2}{\widehat{\alpha}_k}) \cdot |\sigma| + \alpha_0\epsilon_0\mu_2 + \frac{\alpha_0\alpha_n}{\widehat{\alpha}_k}\epsilon_0\mu_2. \tag{141}$$

■

Neglecting all the insignificant terms, the accuracy of the approximation depends on α_0, α_n, ϵ, $\widehat{\alpha}_k$ and $|\sigma|$, as well as the machine precision ϵ_0.

If we choose $\epsilon \approx \alpha_n$ in eq. (129), then $\frac{\alpha_n}{\widehat{\alpha}_k} \leq \frac{\alpha_n}{\epsilon} = 1$ and, accordingly,

$$\begin{aligned}
\|f - \widehat{f}_N\|_{L^\infty[0,1]} &\lesssim \alpha_0 \cdot (\epsilon + \alpha_n) \cdot |\sigma| + \alpha_0\epsilon_0\mu_2 \\
&\approx \alpha_0\alpha_n|\sigma| + \alpha_0\epsilon_0\mu_2.
\end{aligned} \tag{142}$$

Thus, the approximation error can achieve a bound that is roughly proportional to $\alpha_n|\sigma|$. Otherwise, if ϵ is significantly smaller than α_n, then the error will exceed $\alpha_n|\sigma|$ because of the term $\frac{{\alpha_n}^2}{\widehat{\alpha}_k}$.

8 Extension from Measures to Distributions

In section 7, we presented an algorithm for approximating functions of the form

$$f(x) = \int_a^b x^\mu \sigma(\mu)\, d\mu, \qquad x \in [0, 1], \tag{143}$$

where σ is a signed Radon measure, and derived an estimate for the uniform error of the approximation in theorem 7.3. In this section, we observe that this same algorithm can be applied more generally to functions of the form

$$f(x) = \langle \sigma, x^\mu \rangle, \tag{144}$$

where $\sigma \in \mathcal{D}'(\mathbb{R})$ is a distribution supported on the interval $[a, b]$. Since every distribution with compact support has a finite order, it follows that $f \in C^m([a, b])^*$ for some order $m \geq 0$.

Recall that

$$|\langle \sigma, x^\mu \rangle| \leq \|\sigma\|_{C^m([a,b])^*} \cdot \|x^\mu\|_{C^m([a,b])}, \tag{145}$$

where

$$\|x^\mu\|_{C^m([a,b])} = \sum_{n=0}^{m} \sup_{x \in [a,b]} |(x^\mu)^{(n)}|, \tag{146}$$

and

$$\|\sigma\|_{C^m([a,b])^*} = \sup_{\substack{\varphi \in C^m[a,b] \\ \|\varphi\|_{C^m[a,b]}=1}} |\sigma(\varphi)|. \tag{147}$$

We can use the algorithm of section 7 to approximate a function of the form eq. (144), where the approximation error is bounded by the following theorem, which generalizes theorem 7.3.

Theorem 8.1. *Let $f(x)$ be a function of the form eq. (144), for some distribution $\sigma \in C^m([a, b])^*$ of order $m \geq 0$. Suppose that $N = \min\{i : \alpha_i \leq \frac{\alpha_n{}^2}{2\sqrt{n}}\}$. Let $t_1, t_2, \ldots, t_N$ be the roots of u_N shifted to the interval $[a, b]$, and let $x_1, x_2, \ldots, x_N$ be the collocation points defined by formula $x_j = e^{-\frac{s_j}{b-a}}$, where $s_1, s_2, \ldots, s_N$ are the roots of v_N. Suppose $V \in \mathbb{R}^{N\times N}$ is defined in eq. (102) and $F \in \mathbb{R}^N$ is defined in eq. (103), and let $\epsilon > 0$. Suppose further that*

$$\widehat{c}_k = (V + \delta V)_k^\dagger (F + \delta F), \tag{148}$$

where $(V + \delta V)_k^\dagger$ is the pseudo-inverse of the k-TSVD of $V + \delta V$, so that

$$\widehat{\alpha}_k \geq \epsilon \geq \widehat{\alpha}_{k+1}, \tag{149}$$

where $\widehat{\alpha}_k$ and $\widehat{\alpha}_{k+1}$ denote the kth and $(k+1)$th largest singular values of $V + \delta V$, where $\delta V \in \mathbb{R}^{N\times N}$ and $\delta F \in \mathbb{R}^N$, with

$$\|\delta V\|_2 \leq \epsilon_0 \cdot \mu_1 < \frac{\epsilon}{2}, \tag{150}$$

and

$$\|\delta F\|_2 \le \epsilon_0 \cdot \mu_2. \tag{151}$$

Let

$$\widehat{f}_N(x) = \sum_{j=1}^{N} \widehat{c}_{k,j} x^{t_j}, \tag{152}$$

with $\widehat{c}_k$ *defined in eq.* (148)*. Then,*

$$\|f - \widehat{f}_N\|_{L^\infty[0,1]} \lesssim \alpha_0 \cdot (\epsilon + \alpha_n + \frac{{\alpha_n}^2}{\widehat{\alpha}_k}) \cdot \|\sigma\|_{C^m([a,b])^*} \cdot \max_{0\le i\le n-1} \left\|u_i\left(\tfrac{t-a}{b-a}\right)\right\|_{C^m[a,b]} + \alpha_0\epsilon_0\mu_2 + \frac{\alpha_0\alpha_n}{\widehat{\alpha}_k}\epsilon_0\mu_2 \tag{153}$$

Proof. Since the proof closely resembles the one of theorem 7.3, we omit it here. The only difference is that $|\sigma|$ in eq. (129) is replaced by $\|\sigma\|_{C^m([a,b])^*} \cdot \max_{0\le i\le n-1} \left\|u_i\left(\frac{t-a}{b-a}\right)\right\|_{C^m[a,b]}$, due to the fact that

$$|\langle \sigma, u_i\left(\tfrac{t-a}{b-a}\right)\rangle| \le \|\sigma\|_{C^m([a,b])^*} \cdot \left\|u_i\left(\tfrac{t-a}{b-a}\right)\right\|_{C^m[a,b]}, \tag{154}$$

where the term $\left\|u_i\left(\frac{t-a}{b-a}\right)\right\|_{C^m[a,b]}$ is not negligible, for $m \ge 1$. ■

Note that, when σ is a signed Radon measure, the corresponding distribution has order zero, and $\|\sigma\|_{C([a,b])^*} = |\sigma|$. Thus, in this case, the above bound on $\|f - \widehat{f}_N\|_{L^\infty[0,1]}$ is exactly the same as the bound described in eq. (129).

9 Practical Numerical Algorithm

A remarkable result of the experiments in section 5 is that, in practice, functions $f(t) = e^{-x(t+\frac{1}{\gamma-1})} u_i(t)$ can be integrated to precision α_n^2 using only $N = n$ points, and the interpolation matrix $A \in \mathbb{R}^{N\times n}$ defined in eq. (59) is well conditioned, also for $N = n$. As a result, by taking $N = n$, we can establish the same bounds on $\|c\|_2$ and $\|f - f_N\|_{L^\infty[0,1]}$ as those described in theorem 6.1. Furthermore, the fact that A remains well-conditioned for $N = n$ means that eq. (116) in lemma 7.2 still hold. Consequently, we achieve a uniform approximation error of the same size as in eq. (129) in theorem 7.3, for $N = n$.

Previously, we assumed $\epsilon \approx \alpha_n$. When $N = n$, we instead choose ϵ as follows. First, we observe $\|V^{-1}\|_2 \le \frac{1}{\alpha_n}$, as shown in fig. 7. Letting $\widetilde{\alpha}_n$ denotes the n-th singular values of V, and assuming that $\|\delta V\|_2 \le \frac{\widetilde{\alpha}_n}{2}$, we have

$$\|(V + \delta V)^{-1}\|_2 \le \frac{1}{\widetilde{\alpha}_n - \|\delta V\|_2} \le \frac{2}{\widetilde{\alpha}_n} = 2\|V^{-1}\|_2. \tag{155}$$

Thus, $\|(V + \delta V)^{-1}\|_2 \lesssim \frac{1}{\alpha_n}$, which is equivalent to $\frac{1}{\widehat{\alpha}_n} \lesssim \frac{1}{\alpha_n}$. We have then that $\frac{\alpha_n}{\widehat{\alpha}_k} \lesssim 1$, and therefore, as long as ϵ is not larger than α_n, the resulting approximation error is bounded by

$$\begin{aligned}\|f - \widehat{f}_N\|_{L^\infty[0,1]} &\lesssim \alpha_0 \cdot (\epsilon + \alpha_n) \cdot |\sigma| + \alpha_0\epsilon_0\mu_2 \\ &\lesssim \alpha_0\alpha_n|\sigma| + \alpha_0\epsilon_0\mu_2.\end{aligned} \tag{156}$$

In practice, we take $\epsilon = \epsilon_0$.

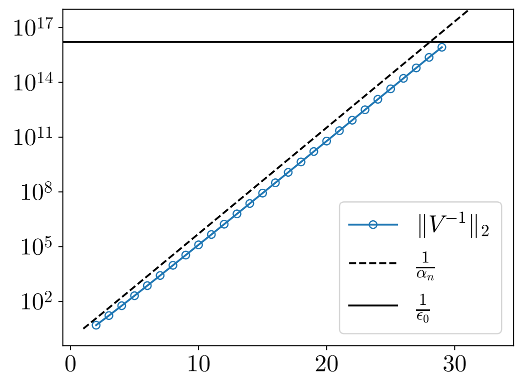

(a) $\gamma = 10$: $a = 1$, $b = 10$

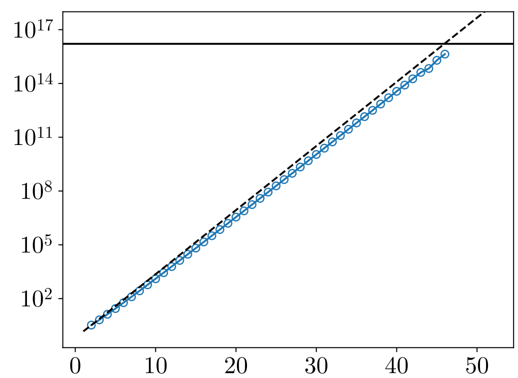

(b) $\gamma = 100$: $a = 1$, $b = 100$

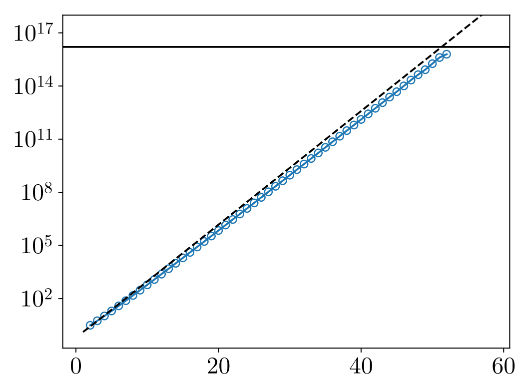

(c) $\gamma = 200$: $a = 1$, $b = 200$

Figure 7: A comparison between $\|V^{-1}\|_2$, and $\frac{1}{\alpha_n}$, for $\gamma = 10,\ 100,\ 200$.

10 Numerical Experiments

In this section, we demonstrate the performance of our algorithm with several numerical experiments. Our algorithm was implemented in Fortran 77, and compiled using the GFortran Compiler, version 12.2.0, with -O3 flag. All experiments were conducted on a laptop with 32 GB of RAM and an Intel 12nd Gen Core i7-1270P CPU.

10.1 Approximation Over Varying Values of n

In this subsection, we approximate functions of the form $f(x) = \int_a^b x^\mu \sigma(\mu)\, d\mu$, $x \in [0,1]$, for the following cases of $\sigma(\mu)$:

$$\sigma_1(\mu) = 1, \tag{157}$$

$$\sigma_2(\mu) = \frac{1}{\mu}, \tag{158}$$

$$\sigma_3(\mu) = \sin(12\mu), \tag{159}$$

$$\sigma_4(\mu) = \sin(12\mu)^2, \tag{160}$$

$$\sigma_5(\mu) = e^{-10\mu}, \tag{161}$$

$$\sigma_6(\mu) = \frac{e^{-10\mu}}{\mu}. \tag{162}$$

We apply our algorithm with $N = n$ and $\epsilon = \epsilon_0$, where ϵ is the truncation point of the TSVD, as described in theorem 7.3. We estimate $\|f - \widehat{f}_N\|_{L^\infty[0,1]}$, by evaluating f and $\widehat{f}_N$ at 2000 uniformly distributed points over $[0,1]$, and finding the maximum error between f and $\widehat{f}_N$ at those points. We repeat the experiments for $\gamma = 10$, 100, 200, and plot $\|f - \widehat{f}_N\|_{L^\infty[0,1]}/|\sigma|$. The results are displayed in figs. 8 to 10.

It is evident that $\|f - \widehat{f}_N\|_{L^\infty[0,1]}/|\sigma|$ remains bounded by α_n, as shown in section 9, until it reaches a stabilized level that is close to the machine precision multiplied by some small constant. Since $\{\alpha_i\}_{i=0,1,\dots,\infty}$ decays exponentially, the approximation exhibits an exponential rate of convergence in N.

10.2 Approximation of Non-integer Powers

In this subsection, we fix $N = n$, where $\alpha_n \approx \epsilon_0$. Our goal is to approximate functions of the form $f(x) = \int_a^b x^\mu \sigma(\mu)\, d\mu$, $x \in [0,1]$, with

$$\sigma_7(\mu) = \delta(\mu - c), \tag{163}$$

where $c \in [a,b]$. The resulting function is $f(x) = x^c$. We approximate such functions for 1000 values of c distributed logarithmically in the interval $[\frac{a}{1.5}, 1.5b]$. We set $\epsilon = \epsilon_0$, and evaluate f and $\widehat{f}_N$ at 1000 uniformly distributed points over $[0,1]$ to estimate $\|f - \widehat{f}_N\|_{L^\infty[0,1]}/|\sigma|$. The results for $\gamma = 10, 100, 200$ are displayed in fig. 11. It can be observed that the approximation error remains accurate up to the machine precision multiplied by some small constants, for values of c within the interval $[a,b]$, and grows significantly, for values of c outside $[a,b]$.

10.3 Approximation in the Case of Distributions

In this subsection, we assume $\sigma \in \mathcal{D}'(\mathbb{R})$ has the form

$$\sigma_8(\mu) = \delta^{(k)}(\mu - c), \tag{164}$$

where $k \geq 0$ is an integer, $c \in [a,b]$, and $\delta(t)$ is the Dirac delta function. The resulting function is $f(x) = x^c(\log x)^k$. We apply our algorithm with $N = n$ and $\epsilon = \epsilon_0$, and evaluate f and $\widehat{f}_N$ at 2000 uniformly distributed points in $[0,1]$ to estimate $\|f - \widehat{f}_N\|_{L^\infty[0,1]}/|\sigma|$.

The results for $k = 1\ 2, \ldots, 6$, $c = a$, $\frac{a+b}{2}$, b, and $\gamma = 10$, 100, 200 are shown in figs. 12 to 14.

In contrast to the previous case where σ is a signed Radon measure, the approximation error can increase significantly with k. However, the approximation error is still bounded by $(\epsilon + \alpha_n) \cdot \max_{0\le i\le n-1} \left\| u_i\left(\frac{t-a}{b-a}\right)\right\|_{C^m[a,b]}$, as stated in theorem 8.1. Furthermore, we observe that the error grows with k, and when $c = a$, the error is closely aligned with the estimated bound, since the function is more singular for smaller c and the approximation error tends to be larger.

10.4 Approximation Over a Simple Arc in the Complex Plane

In this subsection, we investigate the performance of our algorithm on simple and smooth arcs in the complex plane. Suppose that $\widetilde{\gamma}\colon [0,1] \to \mathbb{C}$, and let $\Gamma = \widetilde{\gamma}([0,1])$. We replace the interpolation matrix V in eq. (102) by a modified interpolation matrix V_Γ, defined by

$$V_\Gamma = \begin{pmatrix} \widetilde{\gamma}(x_1)^{t_1} & \widetilde{\gamma}(x_1)^{t_2} & \dots & \widetilde{\gamma}(x_1)^{t_N} \\ \widetilde{\gamma}(x_2)^{t_1} & \widetilde{\gamma}(x_2)^{t_2} & \dots & \widetilde{\gamma}(x_2)^{t_N} \\ \vdots & \vdots & \ddots & \vdots \\ \widetilde{\gamma}(x_N)^{t_1} & \widetilde{\gamma}(x_N)^{t_2} & \dots & \widetilde{\gamma}(x_N)^{t_N} \end{pmatrix} \in \mathbb{C}^{N\times N}. \tag{165}$$

Specifically, we consider the arc $\widetilde{\gamma}(t) = t + \alpha i(t^2 - t)$, for $\alpha = 0.8$, 1.6 and 2.4, which are plotted in fig. 15. Our goal is to approximate functions of the form

$$f_\Gamma(t) := \int_a^b \widetilde{\gamma}(t)^\mu \sigma(\mu)\, d\mu, \tag{166}$$

over the arc $\widetilde{\gamma}(t)$, where $t \in [0, 1]$. We apply the algorithm with $N = n$ and $\epsilon = \epsilon_0$ to the functions $f_\Gamma(t)$ where $\sigma(\mu)$ has the forms $\sigma_1(\mu)$ and $\sigma_5(\mu)$, as defined in eq. (157) and eq. (161), respectively. The experiments are repeated for $\gamma = 10, 100, 200$, and the results are displayed in figs. 16 to 18.

We also investigate the approximation error for non-integer powers $f_\Gamma(t) = \widetilde{\gamma}(t)^c$ over the arc $\widetilde{\gamma}(t)$, where $c \in [\frac{a}{1.5}, 1.5b]$, following the same procedure as the one described in section 10.2. The results are displayed in fig. 19.

By analyzing the approximation error over $\widetilde{\gamma}(t)$, for different values of α, we observe that the approximation error grows with α, and depends on the specific functions being approximated. Generally, when γ is small, the approximation error grows only slightly as the arc becomes more curved, while for large γ, it is possible for the approximation error to grow significantly larger than α_n. When the arc is slightly curved, the approximation performs similarly to the case where $\widetilde{\gamma}(t) = [0, 1]$, with the error bounded by α_n.

10.5 Tapered Exponential Clustering of the Collocation Points

We observe that the collection of collocation points $\{x_j\}_{j=1}^N$ generated by our algorithm exhibits a tapered exponential clustering around the singularity at $x = 0$. Specifically, the density of $\{x_j\}_{j=1}^N$ over $[0, 1]$ tapers in the direction of $x = 0$, when viewed on a logarithmic scale. This observation is demonstrated in fig. 20, for $\gamma = 10$, 100, 200, and for n ranging from 1 to the value of n where $\alpha_n \approx \epsilon_0$.

11 Conclusion

In this paper, we introduce an approach to approximate functions of the form $f(x) = \int_a^b x^\mu \sigma(\mu)\, d\mu$ over the interval $[0, 1]$, by expansions in a small number of singular powers x^{t_1}, x^{t_2}, $\ldots$, x^{t_N}, where $0 < a < b < \infty$ and $\sigma(\mu)$ is some signed Radon measure or some distribution supported on $[a, b]$. Given any desired accuracy ϵ, our method guarantees that the uniform approximation error over the entire interval $[0, 1]$ is bounded by ϵ multiplied by certain small constants. Additionally, the number of basis functions N grows asymptotically as $O(\log \frac{1}{\epsilon})$, and the expansion coefficients can be found by collocating the functions at specially chosen collocation points $x_1, x_2, \ldots, x_N$ and solving an $N \times N$ linear system. In practice, when $\frac{b}{a} = 10$ and σ is a signed Radon measure, our method requires only approximately $N = 30$ basis functions and collocation points in order to achieve machine precision accuracy. Numerical experiments demonstrate that our method can also be used for approximation over simple smooth arcs in the complex plane. A key feature of our method is that both the basis functions and the collocation points are determined a priori by only the values of a, b, and ϵ. This sets it apart from other methods that rely on careful selection of parameters to determine the basis functions. For example, the basis functions used in rational and reciprocal-log approximation are defined by the locations and residues of poles, and the SE-Sinc and DE-Sinc approximations depend on the choices of smooth transformations. Compared to the DE-Sinc approximation, which achieves nearly-exponential rates of convergence at the cost of doubly-exponentially clustered collocation points, our method uses collocation points which exhibit only tapered exponential clustering. Compared to reciprocal-log approximation, which requires the least-squares solution of an overdetermined linear system with many collocation points, our method involves the solution of a small square linear system to determine the expansion coefficients.

Since our method approximates singular functions accurately by expansions in singular powers, it can be used with existing finite element methods or integral equation methods to approximate the solutions of PDEs on nonsmooth geometries or with discontinuous data. Typically, the leading singular terms of the asymptotic expansions of solutions near corners are derived from the angles at the corners, and are added to the basis functions of finite element methods to enhance the convergence rates (see, for example, [29], [7], [23]). Now, with only the knowledge that the singular solutions are of the form eq. (74), we can enhance the convergence rates of finite element methods without knowledge of the angles at the corners, by adding all of the singular powers obtained from our method to the basis functions. Likewise, the singular powers obtained from our method can be used in integral equation methods for PDEs. In integral equation methods, boundary value problems for PDEs are reformulated as integral equations for boundary charge and dipole densities which represent their solutions. Previously, singular asymptotic expansions of the densities, determined by the angles at the corners, were used to construct special quadrature rules to solve these integral equations (see, for example, [24], [25]). Using only the fact that the singular densities are of the form eq. (74), quadrature rules can instead be developed for only the singular powers obtained from our method, independent of the angles at the corners.

References

[1] Babuška, I., B. Andersson, B. Guo, J. M. Melenk, and H. S. Oh. "Finite element method for solving problems with singular solutions." *J. Comput. Appl. Math.* 74 (1996): 51–70.

[2] Bauer, F.L., and C.T. Fike. "Norms and exclusion theorems." *Numer. Math.* 2 (1960): 137–141.

[3] Bertero, M., P. Boccacci, and E.R. Pike. "On The Recovery And Resolution Of Exponential Relaxation Rates From Experimental Data: A Singular-value Analysis Of The Laplace Transform Inversion In The Presence of Noise." *P. Roy. Soc. A-Math. Phy.* 383 (1982): 15–29.

[4] Beylkin, G., and L. Monzón. "On approximation of functions by exponential sums." *Appl. Comput. Harmon. A.* 19 (2005): 1063–5203.

[5] Delves, L.M., and J.L. Mohamed. *Computational Methods for Integral Equations.* Cambridge University Press, 1988.

[6] Filip, S., Y. Nakatsukasa, L. N. Trefethen, and B. Beckermann. "Rational minimax approximation via adaptive barycentric representations." *SIAM J. Sci. Comput.* 40 (2018): A2427–A2455.

[7] Fix, G. J., S. Gulati, and G. I. Wakoff. "On the use of singular functions with finite element approximations." *J. Comput. Phys.* 13 (1973): 209–228.

[8] Gončar, A. A. "On the rapidity of rational approximation of continuous functions with characteristic singularities." *Math. USSR-Sb.* 2 (1967): 561–568.

[9] Gopal, A., and L. N. Trefethen. "New Laplace and Helmholtz solvers." *Proc. Natl. Acad. Sci.* 116 (2019): 10223–10225.

[10] Gopal, A., and L. N. Trefethen. "Solving Laplace Problems with corner singularities via rational functions." *SIAM J. Numer. Anal.* 57 (2019): 2074–2094.

[11] Gutknecht, M. H., and L. N. Trefethen. "Nonuniqueness of best rational Chebyshev approximations on the unit disk." *J. Approx. Theory* 39 (1983): 275–288.

[12] Hansen, P.C. "The truncated SVD as a method for regularization." *BIT* 27 (1987): 534–553.

[13] Lederman, R.R., and V. Rokhlin. "On The Analytical And Numerical Properties Of The Truncated Laplace Transform I." *SIAM J. Numer. Anal.* 53.3 (2015): 1214–1235.

[14] Lederman, R.R., and V. Rokhlin. "On The Analytical And Numerical Properties Of The Truncated Laplace Transform. Part II." *SIAM J. Numer. Anal.* 54.2 (2016): 665–687.

[15] Lehman, R. S. "Developments at an Analytic Corner of Solutions of Elliptic Partial Differential Equations." *J. Math. Mech.* 8 (1959): 727–760.

[16] Lucas, T. R., and H. S. Oh. "The method of auxiliary mapping for the finite element solutions of elliptic problems containing singularities." *J. Comput. Phys.* 108 (1993): 327–342.

[17] Mori, M. " Discovery of the Double Exponential Transformation and Its Developments." for weakly singular Fredholm integral equations of the second kind." *Publ. Res. Inst. Math. Sci.* 41 (2005): 897–935.

[18] Nakatsukasa, Y., and L. N. Trefethen. "An algorithm for real and complex rational minimax approximation." *SIAM J. Sci. Comput.* 42 (2020): A3157–A3179.

[19] Nakatsukasa, Y., and L. N. Trefethen. "Reciprocal-log approximation and planar PDE solvers." *SIAM J. Numer. Anal.* 59 (2021): 2801–2822.

[20] Nakatsukasa, Y., O. Sète, and L. N. Trefethen. "The AAA algorithm for rational approximation." *SIAM J. Sci. Comput.* 40 (2018): A1494–A1522.

[21] Newman, D. J. "Rational approximation to $|x|$. *Mich. Math. J.* 11 (1964): 11–14.

[22] Okayama, T., T. Matsuo, and M. Sugihara. "Sinc-collocation methods for weakly singular Fredholm integral equations of the second kind." *J. Comput. Appl. Math.* 234 (2010): 1211–1227.

[23] Olson, L. G., G. C. Georgiou, and W. W. Schultz. "An efficient finite element method for treating singularities in Laplace's Equation." *J. Comput. Phys.* 96 (1991): 391–410.

[24] Serkh, K. "On the Solution of Elliptic Partial Differential Equations on Regions with Corners." *J. Comput. Phys.* 305 (2016): 150–171.

[25] Serkh, K., and V. Rokhlin. "On the solution of the Helmholtz equation on regions with corners." *Proc. Natl. Acad. Sci.* 113 (2016): 9171–9176.

[26] Stahl, H. "Best uniform rational approximation of x^α on $[0, 1]$." *Acta. Math.* 190 (2003): 241–306.

[27] Stenger, F. "Numerical Methods Based on Sinc and Analytic Functions in numerical Analysis." *SSCM* Springer-Verlag, 1993.

[28] Stenger, F. "Explicit nearly optimal linear rational approximation with preassigned poles." *Math. Comput.* 47 (1986): 225–252.

[29] Tong, P., and T. H. H. Pian. "On the convergence of the finite element method for problems with singularity." *Int. J. Solids Struct.* 9 (1973): 313–321.

[30] Trefethen, L. N., Y. Nakatsukasa, and J. A. C. Weideman. "Exponential node clustering at singularities for rational approximation, quadrature, and PDEs." *Numer. Math.* 147 (2021): 227–254.

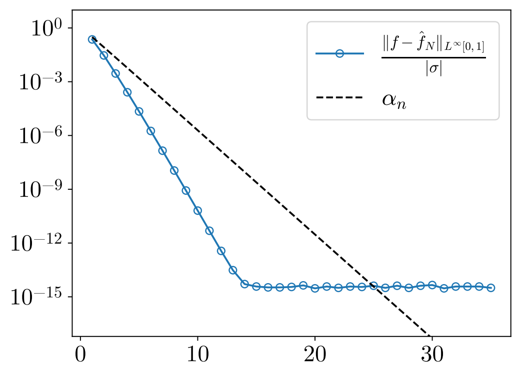

(a) $f(x) = \int_1^{10} x^\mu \sigma_1(\mu)\, d\mu$

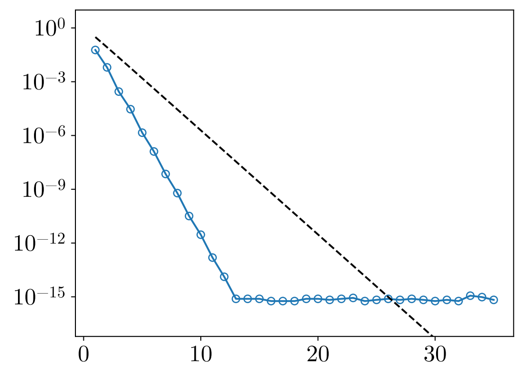

(b) $f(x) = \int_1^{10} x^\mu \sigma_2(\mu)\, d\mu$

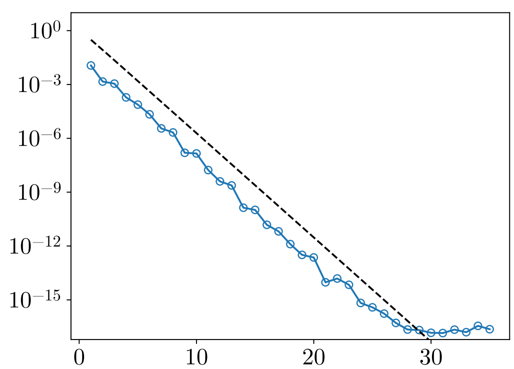

(c) $f(x) = \int_1^{10} x^\mu \sigma_3(\mu)\, d\mu$

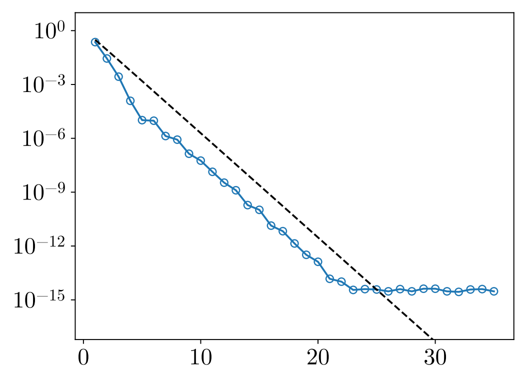

(d) $f(x) = \int_1^{10} x^\mu \sigma_4(\mu)\, d\mu$

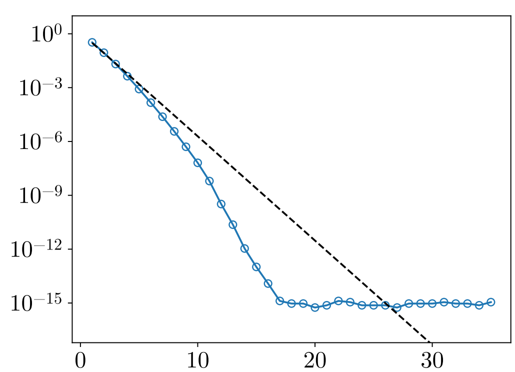

(e) $f(x) = \int_1^{10} x^\mu \sigma_5(\mu)\, d\mu$

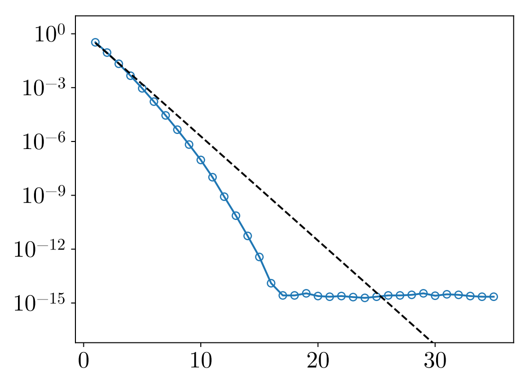

(f) $f(x) = \int_1^{10} x^\mu \sigma_6(\mu)\, d\mu$

Figure 8: The L^∞ approximation error over $[0, 1]$, as a function of n, for $\gamma = 10$.

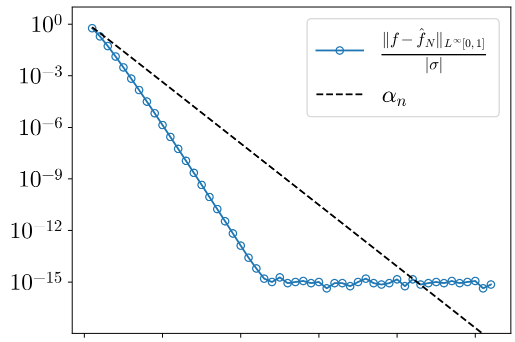

(a) $f(x) = \int_1^{100} x^\mu \sigma_1(\mu)\, d\mu$

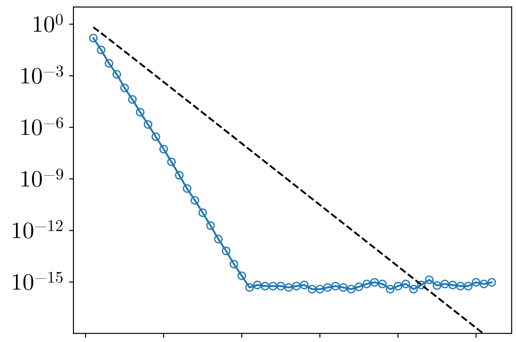

(b) $f(x) = \int_1^{100} x^\mu \sigma_2(\mu)\, d\mu$

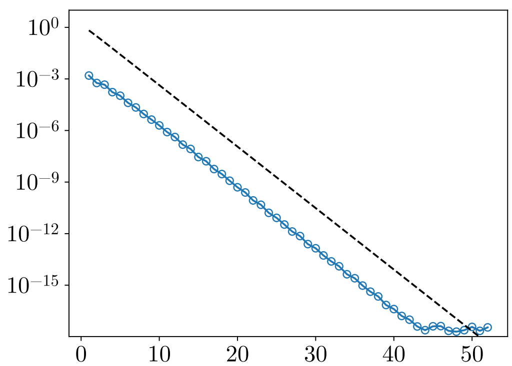

(c) $f(x) = \int_1^{100} x^\mu \sigma_3(\mu)\, d\mu$

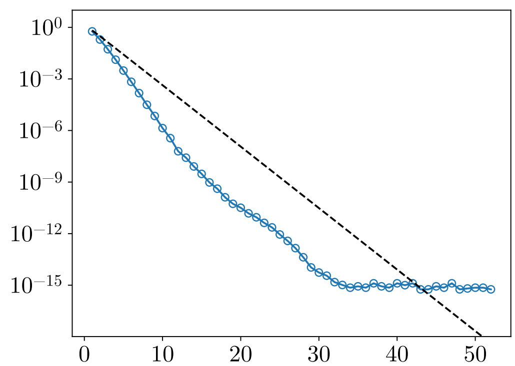

(d) $f(x) = \int_1^{100} x^\mu \sigma_4(\mu)\, d\mu$

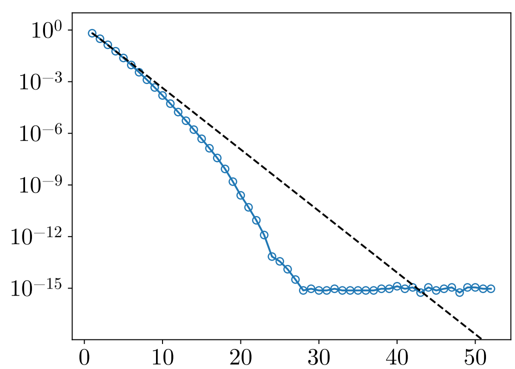

(e) $f(x) = \int_1^{100} x^\mu \sigma_5(\mu)\, d\mu$

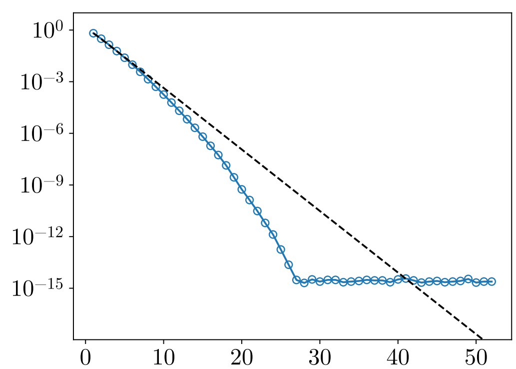

(f) $f(x) = \int_1^{100} x^\mu \sigma_6(\mu)\, d\mu$

Figure 9: The L^∞ approximation error over $[0, 1]$, as a function of n, for $\gamma = 100$.

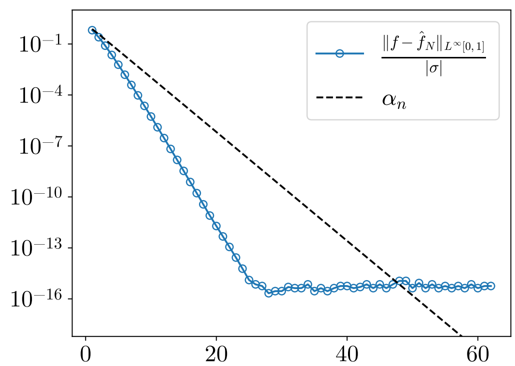

(a) $f(x) = \int_1^{200} x^\mu \sigma_1(\mu)\, d\mu$

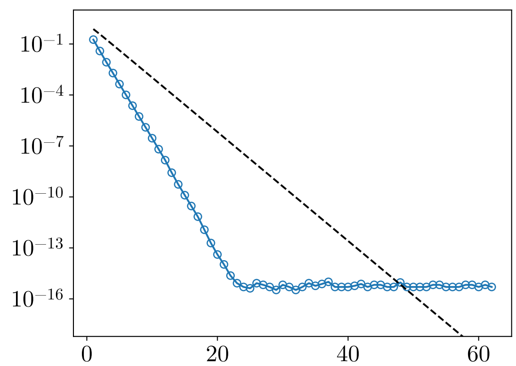

(b) $f(x) = \int_1^{200} x^\mu \sigma_2(\mu)\, d\mu$

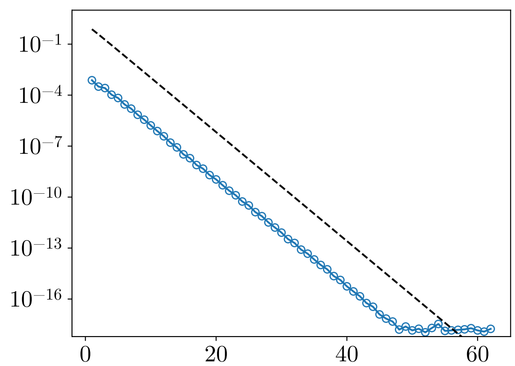

(c) $f(x) = \int_1^{200} x^\mu \sigma_3(\mu)\, d\mu$

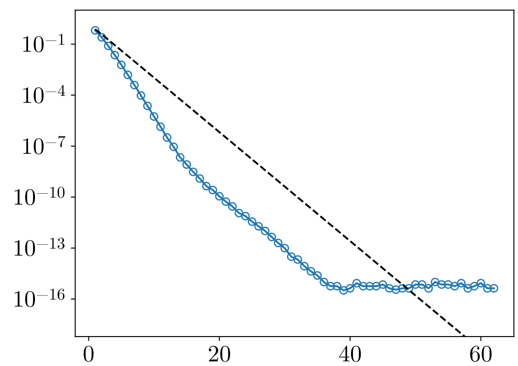

(d) $f(x) = \int_1^{200} x^\mu \sigma_4(\mu)\, d\mu$

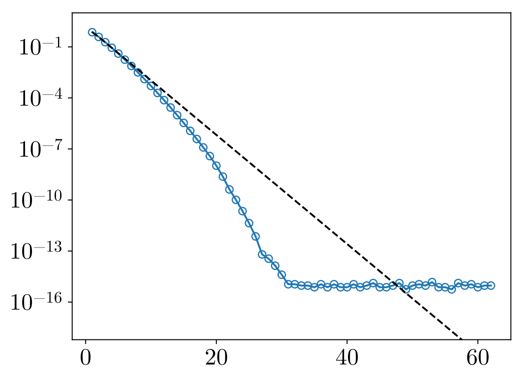

(e) $f(x) = \int_1^{200} x^\mu \sigma_5(\mu)\, d\mu$

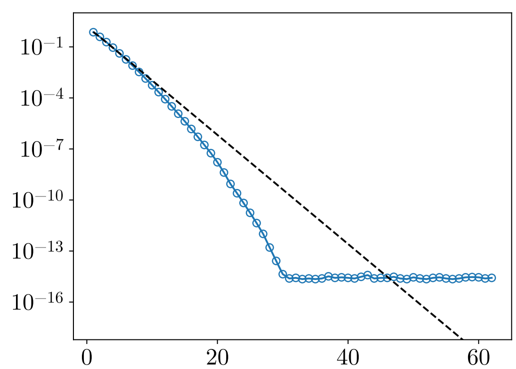

(f) $f(x) = \int_1^{200} x^\mu \sigma_6(\mu)\, d\mu$

Figure 10: The L^∞ approximation error over $[0, 1]$, as a function of n, for $\gamma = 200$.

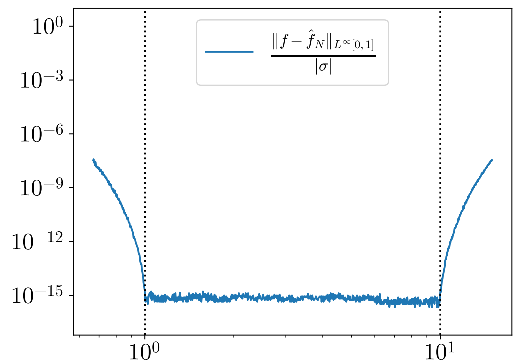

(a) $n = 28$, $\gamma = 10$: $a = 1$, $b = 10$

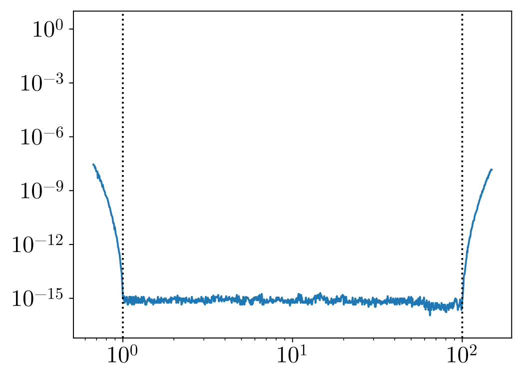

(b) $n = 46$, $\gamma = 100$: $a = 1$, $b = 100$

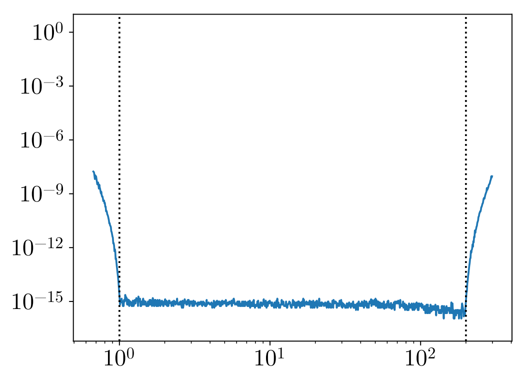

(c) $n = 53$, $\gamma = 200$: $a = 1$, $b = 200$

Figure 11: The L^∞ approximation error of $f(x) = \int_a^b x^\mu \sigma_7(\mu)\, d\mu$, over $[0, 1]$, as a function of c, for a fixed n such that $\alpha_n \approx \epsilon_0$, and for $\gamma = 10$, 100, 200.

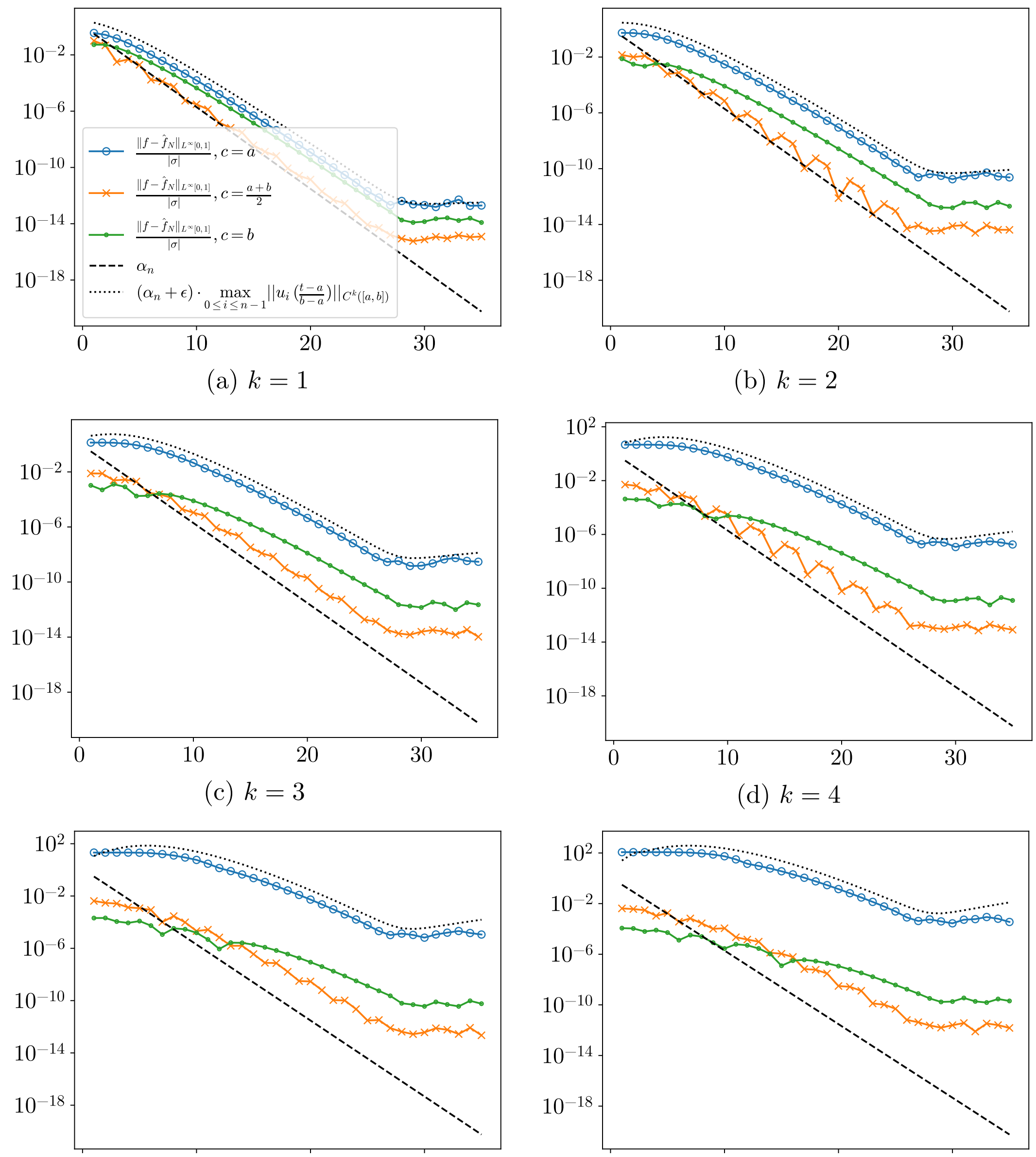

(a) $k = 1$ (b) $k = 2$

(c) $k = 3$ (d) $k = 4$

(e) $k = 5$ (f) $k = 6$

Figure 12: The L^∞ approximation error of $f(x) = \int_1^{10} x^\mu \sigma_8(\mu)\, d\mu$ over $[0, 1]$, as a function of n, for $\gamma = 10$.

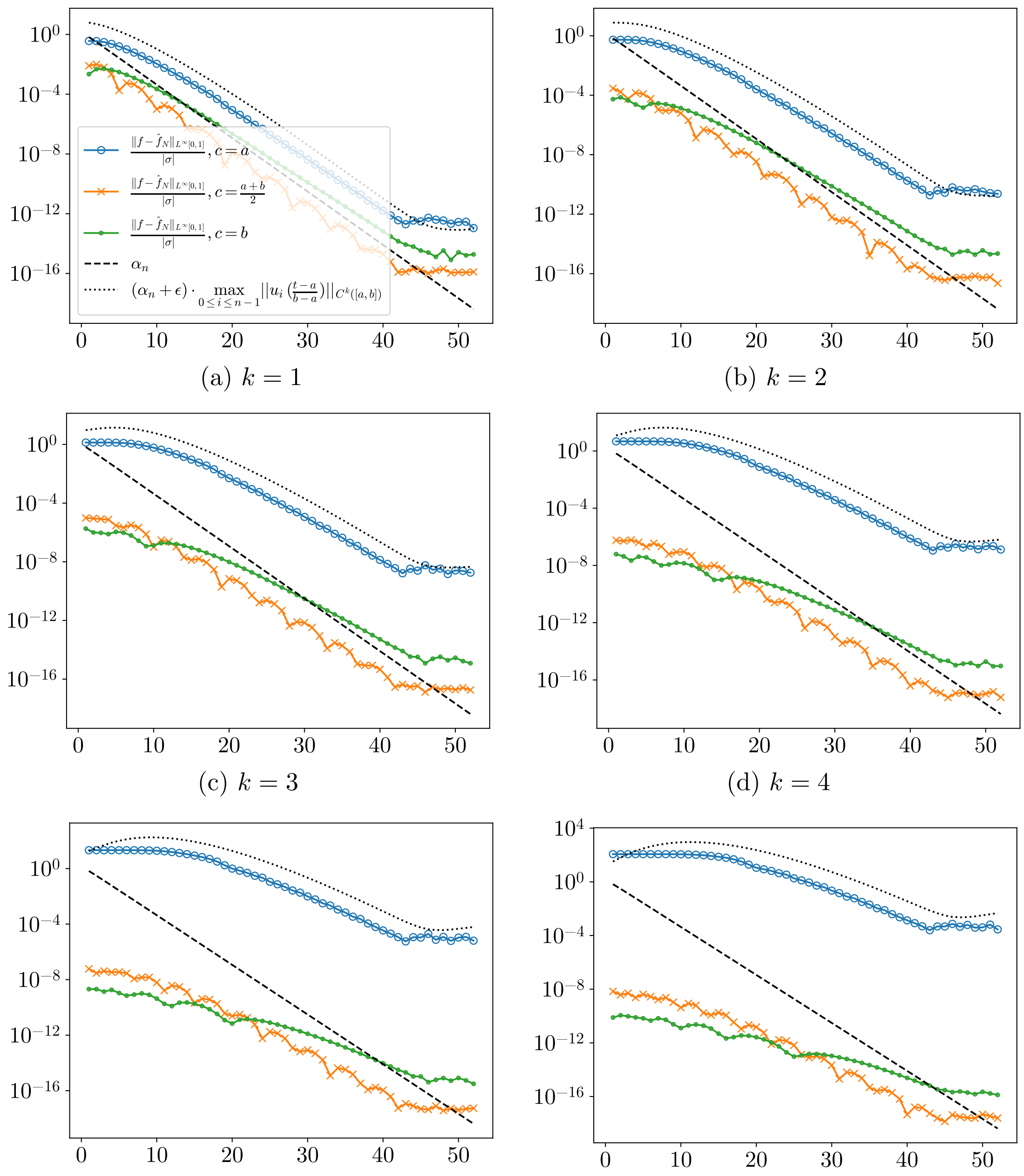

(a) $k=1$ (b) $k=2$

(c) $k=3$ (d) $k=4$

(e) $k=5$ (f) $k=6$

Figure 13: The L^∞ approximation error of $f(x) = \int_1^{100} x^\mu \sigma_8(\mu)\,d\mu$ over $[0,1]$, as a function of n, for $\gamma = 100$.

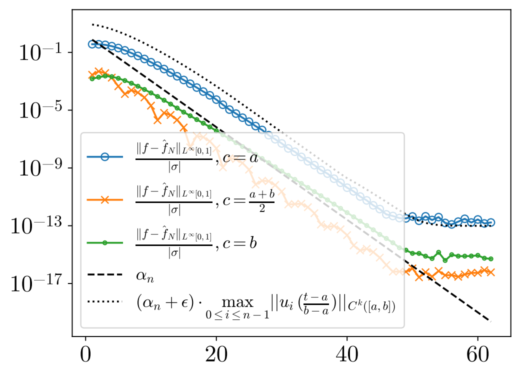

(a) $k = 1$

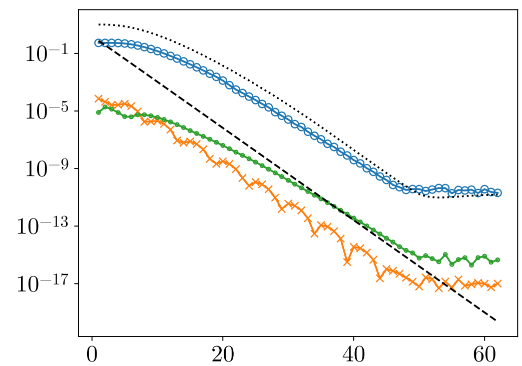

(b) $k = 2$

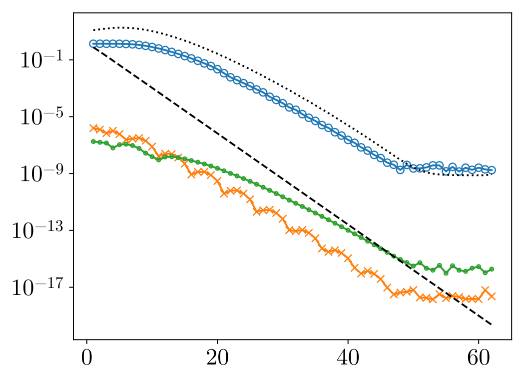

(c) $k = 3$

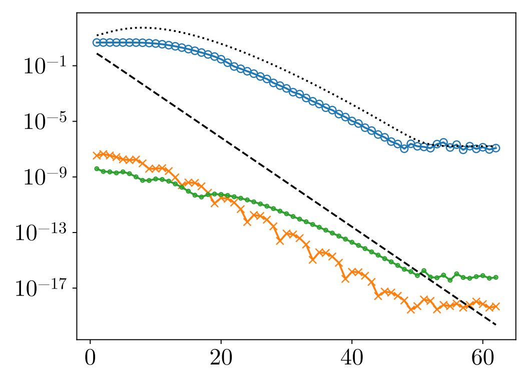

(d) $k = 4$

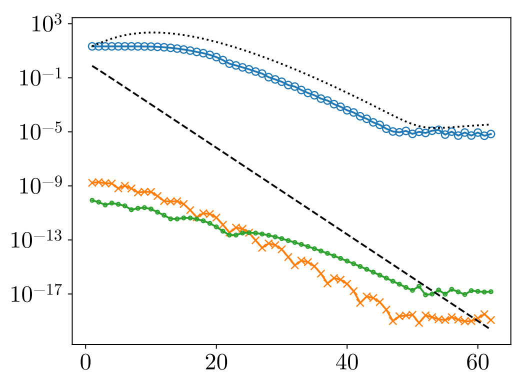

(e) $k = 5$

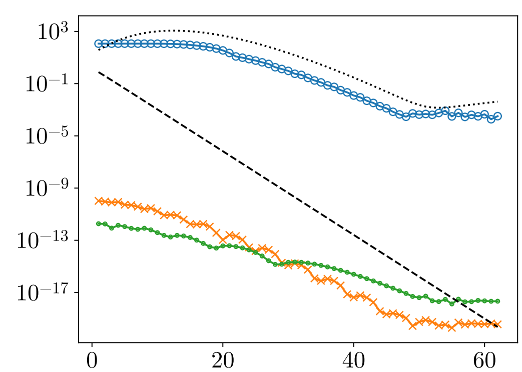

(f) $k = 6$

Figure 14: The L^∞ approximation error of $f(x) = \int_1^{200} x^\mu \sigma_8(\mu)\, d\mu$ over $[0, 1]$, as a function of n, for $\gamma = 200$.

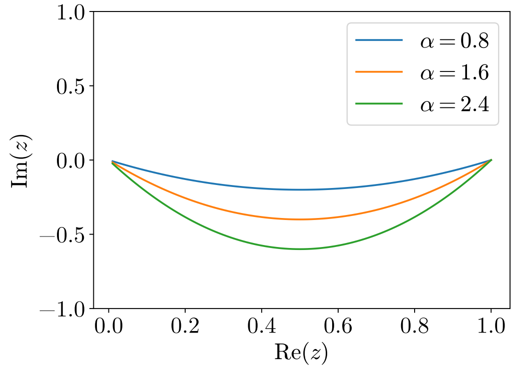

Figure 15: $\widetilde{\gamma}(t) = t + \alpha i(t^2 - t)$.

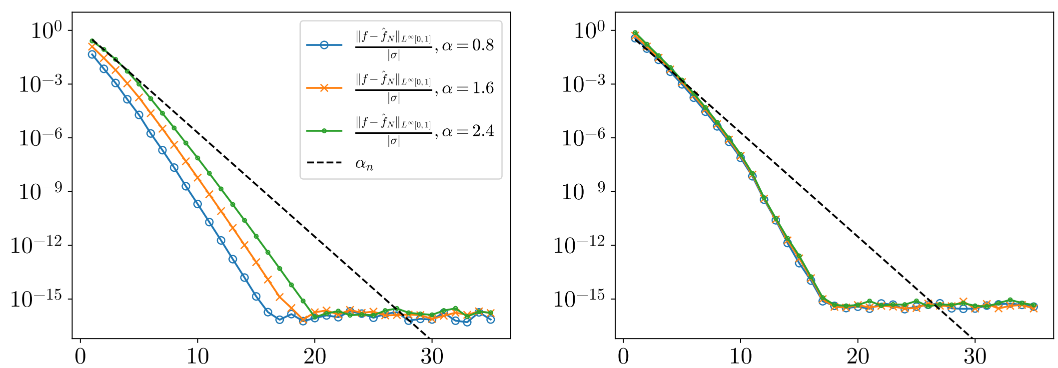

(a) $f_\Gamma(t) = \int_1^{10} \widetilde{\gamma}(t)^\mu \sigma_1(\mu)\, d\mu$

(b) $f_\Gamma(t) = \int_1^{10} \widetilde{\gamma}(t)^\mu \sigma_5(\mu)\, d\mu$

Figure 16: The L^∞ approximation error over $\widetilde{\gamma}(t)$, as a function of n, for $\alpha = 0.8$, 1.6, 2.4, and for $\gamma = 10$.

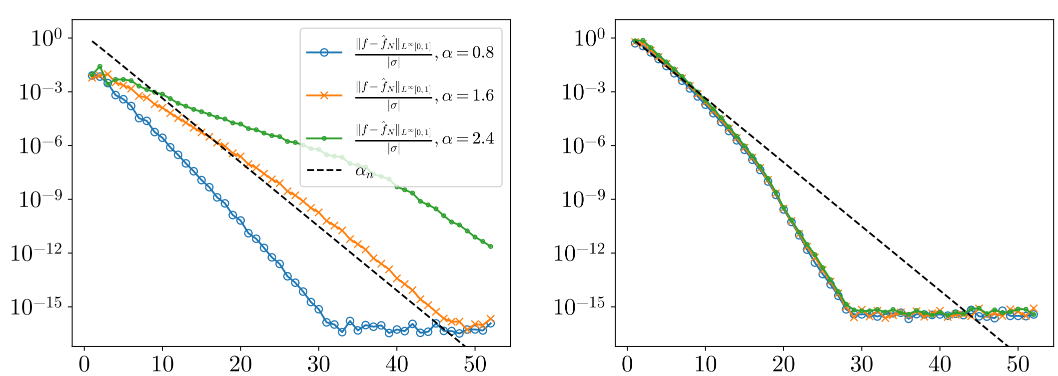

(a) $f_\Gamma(t) = \int_1^{100} \widetilde{\gamma}(t)^\mu \sigma_1(\mu)\, d\mu$

(b) $f_\Gamma(t) = \int_1^{100} \widetilde{\gamma}(t)^\mu \sigma_5(\mu)\, d\mu$

Figure 17: The L^∞ approximation error over $\widetilde{\gamma}(t)$, as a function of n, for $\alpha = 0.8$, 1.6, 2.4, and for $\gamma = 100$.

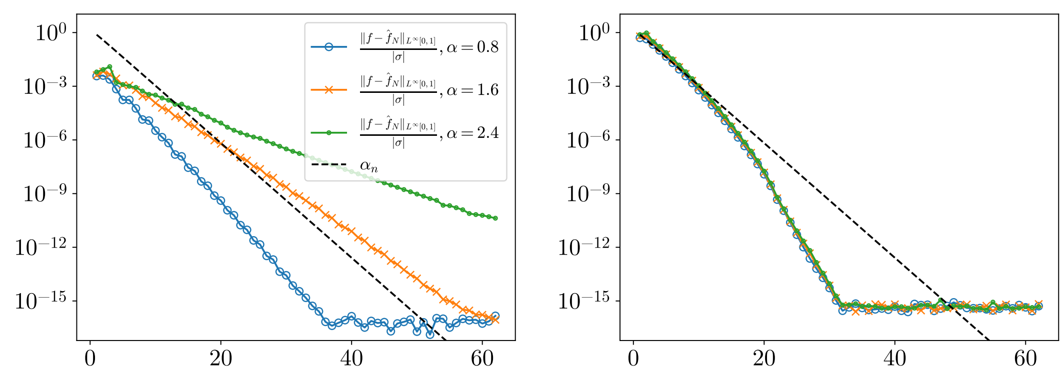

(a) $f_\Gamma(t) = \int_1^{200} \widetilde{\gamma}(t)^\mu \sigma_1(\mu)\, d\mu$

(b) $f_\Gamma(t) = \int_1^{200} \widetilde{\gamma}(t)^\mu \sigma_5(\mu)\, d\mu$

Figure 18: The L^∞ approximation error over $\widetilde{\gamma}(t)$, as a function of n, for $\alpha = 0.8$, 1.6, 2.4, and for $\gamma = 200$.

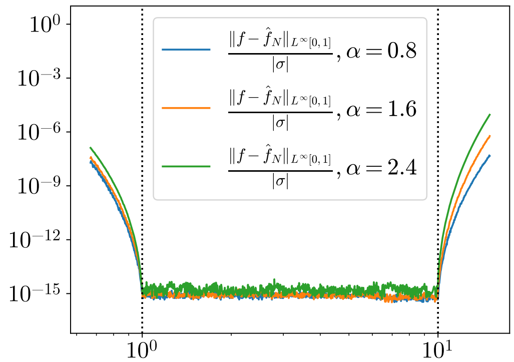

(a) $n = 32$, $\gamma = 10$: $a = 1$, $b = 10$

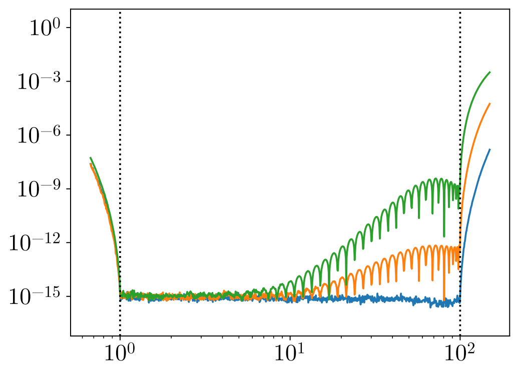

(b) $n = 50$, $\gamma = 100$: $a = 1$, $b = 100$

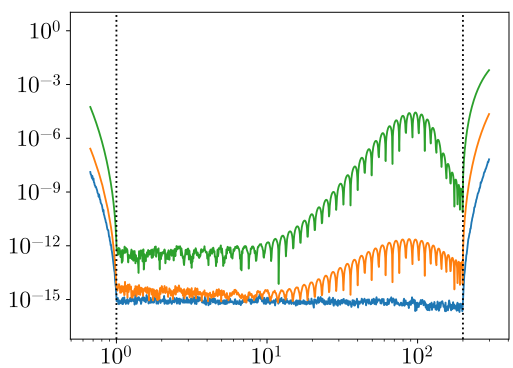

(c) $n = 60$, $\gamma = 200$: $a = 1$, $b = 200$

Figure 19: The L^∞ approximation error of $f_\Gamma(t) = \int_a^b \widetilde{\gamma}(t)^\mu \sigma_7(\mu)\, d\mu$ over $\widetilde{\gamma}(t)$, as a function of c, for a fixed n such that $\alpha_n \approx \epsilon_0$, and for $\gamma = 10$, 100, 200.

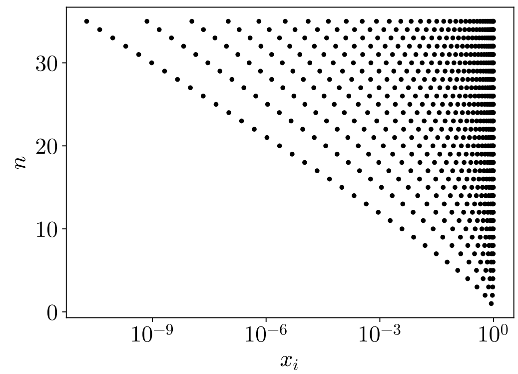

(a) $\gamma = 10$: $a = 1$, $b = 10$

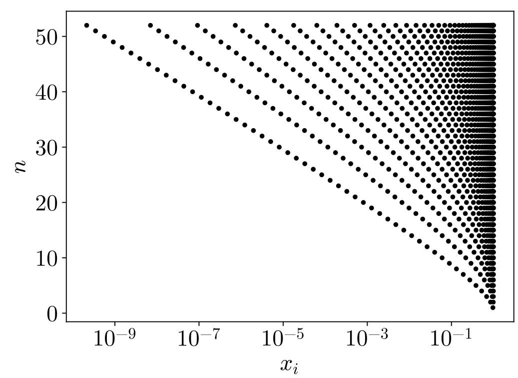

(b) $\gamma = 100$: $a = 1$, $b = 100$

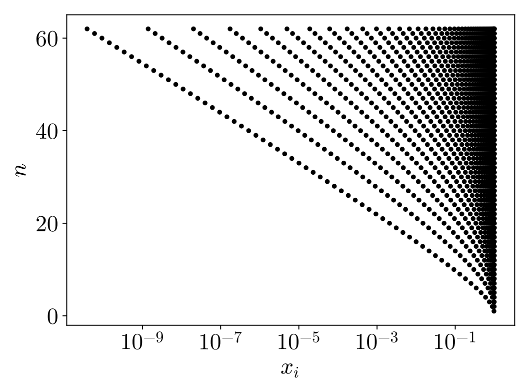

(c) $\gamma = 200$: $a = 1$, $b = 200$

Figure 20: The distribution of collocation points $\{x_j\}_{j=1}^{N}$ over $[0, 1]$, for values of n such that $\alpha_n \gtrsim \epsilon_0$, and for $\gamma = 10$, 100, 200.